Quantum mechanical line widths of ionized oxygen, silicon and aluminium; comparisons with recent experimental results

H Elabidi, S Sahal-Bréchot, Milan S. Dimitrijević, R. Hamdi, W Belhadj

Quantum mechanical line widths of ionized oxygen, silicon and aluminium; comparisons with recent experimental results

H. Elabidi[1]★ , S. Sahal-Bréchot[2] , M. S. Dimitrijević[2,3] , R. Hamdi[4] , W. Belhadj[1]

[1] *Physics Department, College of Applied Science, Umm Al-Qura University, Makkah Almukarramah, Saudi Arabia*
[2] *Observatoire de Paris, PSL University, Sorbonne Université, CNRS, LERMA, 92190 Meudon, France*
[3] *Astronomical Observatory, Volgina 7, 11060 Belgrade, Serbia*
[4] *College of Al-Qunfudah Health Sciences, Umm Al-Qura University, Makkah Almukarramah, Saudi Arabia*

Released 2023 Xxxxx XX

ABSTRACT

We present in this paper new quantum Half Widths at Half intensity Maximum (HWHM) for 101 spectral lines of the following ions: O II (35 lines), O III (20 lines), Si II (9 lines), Si III (12 lines) and Al III (25 lines). The present quantum results are compared to new experimental ones. No previous quantum calculations have been performed for these ions. The relatively high differences found between the new and previous measurements and the available theoretical calculations encourage us to conduct these quantum calculations. Our quantum method has been used many years ago and has given good results compared to other approaches, so it can be a useful tool to check the new experimental results, or to understand the disagreement found for some lines. Furthermore, the obtained results can be used for the abundance determination of elements, the calculation of stellar opacity, the interpretation and modelling of stellar spectra, and the estimation of the relative transfer through stellar plasmas, etc. Part of the present results will be also implemented to the database of Stark broadening parameters STARK-B.

Key words: line:profiles-atomic processes-atomic data-scattering-stars: atmospheres

1 INTRODUCTION

Over the last three decades, the progress of the space astronomy, on the one hand, and the development of computers on the other hand stimulates the stellar spectroscopy that needs a very huge number of elements and line transitions together with their atomic and line broadening data. In fact, many instruments of observations (spectrographs on board or terrestrial telescopes) such as the Far Ultraviolet Spectroscopy Explorer (FUSE) and the Goddard High Resolution Spectrograph (GHRS) on the Hubble Space Telescope, are able to collect a large quantity of spectroscopic data with excellent resolution for plasma with various physical conditions and within different spectral ranges. Furthermore, we become able to produce large amount of atomic data thanks to the development of computers and numerical codes. This combination and complementarity between our needs to data and our ability to produce them (by calculations or observations) open the way to resolve some problems requiring a huge quantity of atomic and line broadening data. As an example of such problems, the calculation of opacities for classical Cepheid models (Iglesias et al. 1990), where approximately 12 millions spectral lines have been considered.

Among the line broadening mechanisms, the Stark broadening -resulting from the action of electric field of particles surrounding an emitter- is the most important. There are two origins of this importance: firstly, because Stark broadening occurs for various physical conditions of plasma, especially for astrophysical plasmas: from clouds of interstellar molecular hydrogen, with temperatures around 30 K and electron densities $N_e = 1-5\,\mathrm{cm}^{-3}$ (conditions that cannot be obtained in laboratory plasmas) to white dwarf atmospheres and hot stars of A and B types with temperature about 10^5 K and density $N_e = 10^{17}\,\mathrm{cm}^{-3}$ (Dimitrijević 2020). The reader can find in Dimitrijević (2003) a set of extremely different plasma conditions for which Stark broadening cannot be neglected. Secondly, the recent discovery of spectral lines emitted by heavy elements (Cu, Zn, Ga, Ge, As, Se, Br, Kr, Sr, Sn, Te, I, etc.) in the ultraviolet (UV) spectra of hot DO white dwarfs such as HD 149499B, PG 0109+111, RE 0503−89 (Werner et al. 2018; Rauch et al. 2020). These astrophysical objects were known before as composed only in hydrogen and helium. The Stark broadening parameters for the spectral lines of these elements must be calculated. New research showed for example the interest of the Fe V ion, and semi classical perturbation calculations of its Stark broadening have been performed (Hamdi et al. 2021). In fact, Rauch et al. (2017) showed that for the spectral analysis of high-resolution of hot stars, accurate atomic and Stark broadening data (measured or calculated) must be provided to perform advanced non-local thermodynamic equilibrium (NLTE)

★ Email: haelabidi@uqu.edu.sa

stellar-atmosphere modelling. Considering only the opacity due to hydrogen and helium in these models leads to inaccurate previsions, and other elements must be included. Besides the spectral analysis (synthesis, analysis, and interpretation of stellar spectra), Stark broadening parameters are required for investigations of radiative transfer through stellar atmospheres; determination of chemical abundances; modelling and investigation of subphotospheric layers. They are also used to investigate the importance of Stark broadening mechanism in plasma conditions of hot DO white dwarfs compared to the Doppler one (Aloui et al. 2022; Sahal-Bréchot & Elabidi 2021). In laboratory plasma applications, Stark broadening data are used in laboratory plasma diagnostics, laser produced plasma and inertial fusion plasma investigation and modelling, the investigations of lasers, and in the research of different technological plasmas, such as those used in laser welding and piercing, as well as for light sources.

This paper deals with Stark broadening of oxygen, aluminium and silicon spectral lines. These three ions are important in astrophysical and laboratory plasmas. Spectral lines emitted by oxygen, aluminium and silicon ions are used in many astrophysical applications: oxygen is the third most abundant element in the universe, after hydrogen and helium, especially, O II and III that are present in many kinds of cosmic light sources. Sollerman et al. (2007) used the O II spectral line emission to determine the star-formation rate and Muzzin et al. (2012) used them to the study of the correlations between the properties of galaxies and their environment and stellar mass. O II and Si III lines have been detected in the spectrum of the bright B-type supergiant HD 306414 (Lorenzo et al. 2014), and have been used to study the radial velocity distribution of interstellar material. Si II and Si III spectral lines were also used in the analysis of magnetic chemically peculiar stars (Khalack & Landstreet 2012). In Sun et al. (2022), the authors presented a sample of four emission-line galaxies at $z = 6:11 - 6:35$ where the O III $\lambda = 500.7$ nm and H_α lines were used to select these sources. Nelson (2000) showed that there is a relationship between nuclear black hole mass (M_{bh}) and the O III spectral line widths for active galactic nuclei (AGNs). The two O III lines ($\lambda\lambda = 436.3, 500.7$ nm) have been detected in the planetary nebula NGC 2440 (Cuesta & Phillips 2000). The experimental evaluations of O III line broadening started since 1931 (Pretty 1931), where the line shifts have been measured. After that, many works have been dedicated to Stark broadening (Platiša et al. 1975; Purić et al. 1988; Blagojević et al. 2000; Srećković et al. 2001b, 2005). Several theoretical studies have been carried out, we can quote the modified semi empirical (Dimitrijević 1988; Dimitrijević & Konjević 1980) and the impact semi classical perturbation theory and calculations: the semi-classical perturbation theory, with hyperbolic trajectories for ionised radiating atoms has been developed and updated by Sahal-Bréchot (1969a,b); Sahal-Bréchot (1974); Fleurier et al. (1977); Sahal-Bréchot (2021): the resulting SCP code has been continually improved and used since 1984 (for example Dimitrijević et al. (2011)). The theory was revisited by Sahal-Bréchot et al. (2014); Sahal-Bréchot & Elabidi (2021). Especially, The calculations using the SCP code has been used in Srećković et al. (2001b); Dimitrijević et al. (2011), but the results presented in Srećković et al. (2001a) are taken from the semi classical tables of Griem (1974). Silicon spectral lines can also be used for the investigation of the solar atmosphere (Lambert & Warner 1968), or for the determination of the luminosity class of a star (Arellano Ferro et al. 2001). An illustrative example of the use of Si II lines is given by the role of the two Si II lines $\lambda\lambda = 412.805; 413.089$ nm in the analysis of the spectra of He-weak stars (Glagolevskij et al. 2006). A list of the papers dealing with the experimental works of O II, Si II and Si III ions can be found in Gavanski et al. (2016). Spectral lines emitted by oxygen, aluminium and silicon ions are also used in laboratory plasma diagnostic such as the determination of electron density, since they often appear as impurities from the glass walls of the discharge tubes (Gavanski et al. 2016). References dealing with the ion Al III are rather less than those of oxygen and silicon. The first detection of Al III absorption was against the halo star HD 18100 (Hartquist et al. 1983). The reason to consider Al III here is the first and the recent measurements of the Stark broadening of its lines (Dojić et al. 2020). The only experimental work on Stark broadening of Al III lines before that of Dojić et al. (2020) was reported in Chan et al. (1996), where only two lines were considered: $\lambda\lambda = 360.0; 570.0$ nm.

Measurements and calculations of line widths are always requested to confirm each other. Unfortunately, we did not reach the stage that the agreement between them is sufficient, even for simple atoms. Comparisons yield varied agreement or disagreement between experimental results or calculations. Measurements have to be performed many times using different procedures and with different experimental set-up, and calculations also must be carried out with different approaches, so that we can check the theoretical methods and the approximations used in the calculations, and at the same time, we can review and revisit the experimental results. Extensive comparisons between consistent Stark broadening results obtained by different methods (experimental or theoretical) can help to decide about the accuracy of the results. This mutual check ensures the improvement of both experimental and theoretical results, and help astrophysicists which results should be considered in their stellar-atmosphere models. Measurements are sometimes guided or encouraged by the available calculations, and on the other hand, new and improved measurements invite us to perform calculations in order to validate the used methods and approaches.

Recently, Gavanski et al. (2016) have carried out new measurements for O II, Si II and Si III spectral line widths at electron temperature $T = 1.5 \times 10^4$ K and electron density $T = 1.45 \times 10^{17}$ cm^{-3}: 37 lines of O II, 10 Si II lines and 12 Si III lines. Some of these lines were measured for the first time. In Gavanski et al. (2016), the plasma was produced in a small electromagnetically driven T-tube (Djurović et al. 2005, 2009, 2015; Gigosos et al. 2014). The T-tube, which is a glass T-shaped tube, with an internal diameter of 27 mm, was filled with pure helium up to 300 Pa. The distance between the reflector and the electrodes was 140 mm. For the discharge, a capacitor bank of 4 μF capacity was charged up to 20 kV. The initialization of the discharge was performed by means of an 11–kV trigger pulse and the current discharge was monitored by a Rogowski coil and an oscilloscope. The spectral lines of O II appear in the 370–490 nm wavelength region, the lines of Si II in the 380–640 nm region, and those of Si III appear in the 300–570 nm region. Gavanski et al. (2016) determined the electron density from the distance between the peaks of the He I line (447.15 nm) using the formula of Ivković et al. (2010), and the electron temperature using the Boltzmann plot of some O II and Si II lines. The measurements of Al III line widths were performed by Dojić et al. (2020) at electron temperature $T = 2.8 \times 10^4$ K and electron density $T = 4.86 \times 10^{17}$ cm^{-3} for 8 spectral lines. Besides the Al III line widths, Dojić et al. (2020) presented also Al II and He I (388.86 nm) line widths. We consider here only the results of Al III because they were measured for the first time. Flat aluminium sample (purity 99.9 per cent) was placed into a home made chamber evacuated by a mechanical vacuum pump. The chamber was mounted on computer controlled x-y-z translation stage to prevent cratering of the sample. The plasma was created by a focused laser pulse from

Nd:YAG, EKSPLA NL311-SH-TH laser. The experiment was conducted in helium-hydrogen gas mixture (92 per cent He, 8 per cent H) in the flowing regime under pressure of 300 mbar (Dojić et al. 2020). These new measurements, and the deviations found between the available results (experimental and theoretical) motivate us to perform in the present work quantum mechanical calculations of Stark broadening for O II, O III, Si II, Si III and Al III spectral lines. The goal is to carry out extensive comparisons with the available experimental and other theoretical results, and participate in testing their accuracy. This is the first time that quantum mechanical calculations for these ions are carried out. Previously, there are the semi classical (Griem 1968), the modified semi empirical (Dimitrijević & Konjević 1980), the simplified modified semi empirical (Dimitrijević & Konjević 1987), and the semi classical perturbation (Dimitrijević & Sahal-Bréchot 1993) calculations.

To calculate the Stark line widths of the considered ions, we have used our quantum mechanical method (Elabidi et al. 2004, 2008). This method has been applied many times (Elabidi & Sahal-Bréchot 2018; Aloui et al. 2018; Elabidi & Sahal-Bréchot 2019; Aloui et al. 2019b,a) and has given good results compared to other approaches. It has been used also to study several physics problems like fine structure effects (Elabidi et al. 2009), strong collisions and quadrupolar potential contributions to Stark broadening (Elabidi et al. 2014), scaling of line widths with temperature and ionic charge (Elabidi & Sahal-Bréchot 2018; Elabidi & Sahal-Bréchot 2019; Elabidi 2021a). In Elabidi (Elabidi 2021a), the calculation of new Stark broadening of about 160 lines for eight neon-like ions, and the investigation of the systematic trend of Stark broadening w with the spectroscopic charge Z, allowed us to establish a linear relation between $\log(w)$ and $\log(Z)$. Using this relation, we could predict the considered line widths for all the Ne-like ions between Mg III and Br XXVI. Our method has been also used to provide new Stark broadening data requested for astrophysical applications (Elabidi 2021b; Sahal-Bréchot & Elabidi 2021; Aloui et al. 2022). In each line broadening calculations, we always evaluate the atomic data used in that calculations to ensure an acceptable accuracy of the results. In the whole paper, Stark half width means half width at half intensity maximum (HWHM).

2 THEORY AND COMPUTATIONAL PROCEDURE

2.1 Overview

Our quantum method for electron impact broadening is well described in (Elabidi et al. 2004, 2008; Aloui et al. 2018). We present here just a brief description. In Elabidi et al. (2004, 2008), we have taken into account fine structure effects and relativistic corrections resulting from the non validity of the LS coupling approximation for the target by using the intermediate coupling schema. We have deduced the following formula of the Half Width at Half intensity Maximum (HWHM) w expressed in angular frequency units of a spectral line arising from a transition from an upper level i to a lower one f:

$$w = N_e \left(\frac{\hbar}{m}\right)^2 \left(\frac{m\pi}{2k_B T}\right)^{\frac{1}{2}} \int_0^\infty \Gamma^w_{i\longmapsto f}(\epsilon) \exp\left(\frac{-\epsilon}{k_B T}\right) \mathrm{d}\left(\frac{\epsilon}{k_B T}\right), \quad (1)$$

where m is the electron mass, k_B the Boltzmann constant, N_e the electron density, T the electron temperature, ϵ the incident electron energy, and

$$\Gamma^w_{i\longmapsto f}(\epsilon) = \sum_{\substack{J_i^T J_f^T \\ l K_i K_f}} \frac{(2K_i+1)(2J_i^T+1)(2K_f+1)(2J_f^T+1)}{2} \times \left\{ \begin{array}{cc} J_i K_i l \\ K_f J_f 1 \end{array} \right\}^2 \left\{ \begin{array}{cc} K_i J_i^T s \\ J_f^T K_f 1 \end{array} \right\}^2 \times \left[1 - \left(\Re(\mathbb{S}_i)\Re(\mathbb{S}_f) + \Im(\mathbb{S}_i)\Im(\mathbb{S}_f)\right)\right]. \quad (2)$$

The momentum coupling schema is defined as follows: the two angular momenta of the emitter (orbital L_j) and (spin S_j) are first coupled to give J_j. This last one is then coupled to orbital momentum l of the colliding electron to give K_j, and finally K_j is coupled with s, the spin of the electron to give the total angular momentum J_j^T $(j = i/f)$ of the system electron-emitter. $\mathbb{S}_j$, $\Re(\mathbb{S}_j)$ and $\Im(\mathbb{S}_j)$ are the scattering matrix elements and their real and imaginary parts for the level j. These matrices are written in the base of the intermediate coupling schema and evaluated at the same colliding energy $\epsilon = \frac{1}{2}mv^2$. $\left\{ \begin{array}{cc} abc \\ def \end{array} \right\}$ are the 6–j symbols.

To evaluate the expression (2) of $\Gamma^w_{i\longmapsto f}$, we need to calculate $\Re(\mathbb{S})$ and $\Im(\mathbb{S})$ in the initial i and final f levels. This task is performed using the UCL codes: SUPERSTRUCTURE (SST) of Eissner et al. (1974) for the structure calculations (energy levels, oscillator strengths...) in addition to the Term Coupling Coefficients (TCCs) which will be used in the scattering part (Elabidi et al. 2004) through the codes DISTORTED WAVE (DW) of Eissner (1998) and JAJOM (Saraph 1978). In the present work, we have transformed JAJOM into JAJPOLARI (Elabidi & Dubau, unpublished results) and RTOS (Dubau, unpublished results) to produce the real $\Re(\mathbb{S})$ and the imaginary $\Im(\mathbb{S})$ parts of the scattering matrix entering our code to evaluate the expression (2). We include in our calculations Feshbach resonances using the Gailitis method (Gailitis 1963). The factor $\Gamma^w_{i\longmapsto f}$ is extrapolated below the threshold energy for the corresponding inelastic process. Considering Feshbach resonances improves the agreement with experimental results, especially for low temperature (Elabidi et al. 2009).

2.2 Discussions of some points about our calculation method

The important contribution of our quantum mechanical method is the treatment of the contribution of strong/elastic collisions to Stark broadening. Firstly, it has been shown in Dimitrijevic et al. (1981) that collisions with $l < 2$ are preponderant and their contributions to widths are important. Furthermore, these collisions occur for low temperature. They showed also that the semi classical and quantum Stark broadening results present the higher disagreement for low temperature, i.e. when the contributions of strong and elastic collisions are dominant. Recently (Elabidi et al. 2014; Aloui et al. 2018; Elabidi 2021b), we deeply investigated this point through quantum and semi classical perturbation calculations of different ions (Ar XV, Ar VII, Br VI, Kr V-VII). We showed that, firstly the strong/elastic collisions effect is high for low temperature. Secondly, when the contributions of strong/elastic collisions to Stark broadening are important, the disagreement with the semi classical perturbation calculations is high and we need to use quantum mechanical calculations to correctly take into account of these effects. As an illustration, we confirm this conclusion for the Al III ion. In Elabidi (2021b); Sahal-Bréchot & Elabidi (2021) we showed that the approximate formula of Cowley (1971), used sometimes by the

astrophysicists when line broadening data are missing, is not adequate for wide temperature scale, and so, we need more accurate calculations. Since 2009, we included in our quantum method the Feshbach resonances (Elabidi et al. 2009), which improve the agreement with experimental results, especially for low temperature.

There are three stages of our calculations for which convergence of the results must be checked: (i) the integral over the incident electron in expression (1), (ii) the sum over the angular momentum l in expression (2) and (iii) the number of electronic configurations and consequently the number of perturber levels at the stage of the atomic structure calculation:

(i) The integral over the energy ϵ is supposed to be carried out from 0 to ∞. For very low energy, the Gailitis method, described before, is used. Here, the integral is numerically performed using the trapezoid method with uniformly increased step. The integration method was tested many times (Elabidi et al. 2004, 2008) and it is easy to check the convergence during the calculations, the process is then stopped when we reach the convergence of this integral.

(ii) The term $\Gamma^{w}_{i\longmapsto f}(\epsilon)$ is principally a sum over l of the scattering matrices $\mathbb{S}$. The contribution of each l to collision strengths (or cross sections) has been investigated many times (Elabidi et al. 2012; Elabidi & Sahal-Bréchot 2013; Ben Nessib et al. 2005), and in our case $l = 19$ is enough for the convergence of the summation.

(iii) The number of perturber levels required for the convergence of the width and the shift of a spectral line has been investigated in Roberts (1968) for the semi classical method. It has been shown that about thirteen levels are required for the convergence of width, and the use of less levels may particularly affect the shift. We note that the configurations used in our structure calculations yield: 70 levels for O II, 41 levels for O III, 61 levels for Si II, 46 levels for Si III and 13 levels for Al III. So we can be sure about the convergence of our calculations of Stark widths.

2.3 Checking the impact and the ideal plasma approximations

Before presenting and discussing our results, it is useful to give an idea about the validity conditions of the main approximations used in this work, especially the impact approximation and the ideal plasma approximation. The first approximation is the base of the Baranger's theory, and the second one allows us to deduce the Stark broadening w for other densities using a linear relationship between w and N_e (for a given temperature).

2.3.1 *The impact approximation*

The impact approximation states that the emitter interacts with only one perturber at the same time, so the duration τ of an interaction must be much smaller than the mean interval time Δt between two successive collisions (Baranger 1958): $\tau \ll \Delta t$, where Δt is of order of the inverse of collisional line width w. The condition of impact approximation can be written

$$w\tau \ll 1. \tag{3}$$

Writing the mean typical velocity v_{typ} of the incident electron as approximately equal to $\frac{\rho_{typ}}{\tau}$, where ρ_{typ} is a typical impact parameter, the duration of an interaction is $\tau \approx \frac{\rho_{typ}}{v_{typ}}$. The collisional line width w can be roughly expressed as $N_e v_{typ} \rho^2_{typ}$. Thus, the validity condition of the impact approximation can be written as

$$\rho^3_{typ} \ll N_e^{-1}, \tag{4}$$

where ρ^3_{typ} is called the 'collision volume'. If we relate the classical orbital momentum of the perturber $l = \rho m v$ to the eigenvalues of the corresponding quantum-mechanical operator $\mathbf{L}^2$ by $L^2 = (\rho m v)^2 = \hbar^2 l(l+1)$, and express the velocity (averaged over the Maxwell-Boltzmann distribution) as $v = \sqrt{8k_BT/\pi m}$, then a typical 'collision volume' is (with $T_{typ} = 10^4$ K and $l_{typ} = 19$):

$$\rho^3_{typ} = \left(\frac{\pi l^2_{typ}\hbar^2}{8mk_BT_{typ}}\right)^{3/2} = 4.43\times10^{-20}\mathrm{cm}^3. \tag{5}$$

With $N_e = 10^{17}$ cm^{-3}, we find $\rho^3_{typ} \ll N_e^{-1}$. Consequently, the impact approximation is valid for the electron density interval $[10^{17}, 10^{18}]$ cm^{-3} considered in the present work.

2.3.2 *The ideal plasma approximation*

The criterion of the ideal plasma approximation is based on the concept of Debye length (or Debye radius) R_D, which is defined in plasma physics as the distance over which electric charges screen out the electric fields:

$$R_D = \sqrt{\frac{\varepsilon_0 k_B T}{N_e e^2}} \tag{6}$$

where ε_0 is the permittivity of free space and e is the elementary charge in S.I. units. To keep a plasma ideal, the number of perturbers N_D inside the Debye sphere of radius R_D must be greater than 1 ($N_D = N_e V > 1$).
With $V = \frac{4\pi}{3}R_D^3$ being the volume of the Debye sphere, we find

$$N_e(\mathrm{cm}^{-3}) < 1.9\times10^6 T^3(\mathrm{K}). \tag{7}$$

Taking the lowest temperature $T = 10^4$ K, we find that $N_e \lesssim 2\times10^{18}$ cm^{-3}. Therefore, with the density $N_e \approx 10^{17}$ cm^{-3}, our plasma can be considered as ideal for the used temperatures, and consequently, Stark broadening can be deduced for lower densities using a linear relationship between W and N_e (for a given temperature).The inequality (7) shows that for the other temperatures greater than 10^4 K, the accepted values of density will increase and reach $N_e = 4\times10^{20}$ cm^{-3} for the highest temperature $T = 6\times10^4$ K.

3 RESULTS AND DISCUSSIONS

3.1 Results for O II

The singly ionized oxygen is a nitrogen-like ion. We used in our structure and collision study five electronic configurations: $1s^2(2s^22p^3$, $2s2p^4$, $2s^22p^23s$, $2s^22p^23p$, $2s^22p^23d)$ yielding to 70 fine structure levels. The scaling parameters λ_l provided by the code SST are $\lambda_s = 1.3022$, $\lambda_p = 1.2231$, and $\lambda_d = 1.1592$. We calculated the Stark broadening of 35 spectral lines arising from 16 multiplets belonging to the two transition arrays 3s−3p and 3p−3d. The existing theoretical results are obtained from the semi classical (Griem 1974), the modified semi empirical (Dimitrijević & Konjević 1980) and the simplified modified semi empirical (Dimitrijević & Konjević 1987) calculations. The two last results have been calculated in Gavanski et al. (2016), and they will be denoted G(MSE) and G(SMSE), since there are other MSE and SMSE calculations which are not performed in Gavanski et al. (2016). With the high spread of the existing data, we thought that considering the quantum

calculations, together with the other ones, may improve the theoretical results, and help us concluding about the degree of agreement between measured and calculated Stark broadening. The experimental results included in the comparisons are those of Platiša et al. (1975); Purić et al. (1988); Djeniže et al. (1991, 1998); Del Val et al. (1999); Blagojević et al. (1999); Srećković et al. (2001a), and the recent experiments of Gavanski et al. (2016).

We present in Table 1 our Stark half widths at half intensity maximum (HWHM) w_Q, the semi classical w_{Gr} (Griem 1974) and the results of Gavanski et al. (2016): $w_{G(MSE)}$ obtained by using the modified semi empirical (Dimitrijević & Konjević 1980) and $w_{G(SMSE)}$ obtained by using the simplified modified semi empirical (Dimitrijević & Konjević 1987) methods, all of them are compared to the measured ones w_m. The averaged relative difference between our quantum results and the measured ones is about 9 per cent (for all the lines and all the temperature values). The semi classical results of Griem (1974) present the same difference, however the G(MSE) and the G(SMSE) results of Gavanski et al. (2016) present a difference of about 35 per cent. The measurements of Del Val et al. (1999) and Purić et al. (1988) present the highest difference with our quantum results. We see that the Stark widths of the two lines $2p^2(^3P)3p\ ^4D^\circ_{5/2}-2p^2(^3P)3d\ ^4F_{7/2}$ (λ = 407.216 nm) and $2p^2(^3P)3p\ ^4D^\circ_{5/2}-2p^2(^3P)3d\ ^4F_{5/2}$ (λ = 408.511 nm) present the highest disagreement with the experimental results, and Δ_Q is about 26 per cent. This can be due to the fact that, since the levels $2p^2(^3P)3d\ ^4F_{7/2}$ and $2p^2(^3P)3d\ ^4F_{5/2}$ are belonging to the last (highest) configuration, so the set of the perturbing levels of these two levels -used in the calculation of the scattering matrices in Eq. (2)- is not complete.

Figure 1 shows the relative difference Δ_X between the experimental results and the theoretical ones (including our quantum results) for a set of O II lines (first part of Table 1). We see that almost all our quantum and the semi classical results of Griem (1974) agree with the experimental ones within 0 – 15 per cent. The results in the Figure 1 are averaged over all the lines and the temperature values. The relative errors for the modified and simplified modified semi empirical results are above 15 per cent.

As an illustration, we display in Figure 2 the Stark HWHM of the O II $2p^2(^3P)3s\ ^2P_{3/2}-2p^2(^3P)3p\ ^2D^\circ_{5/2}$ line, where the quantum and the other theoretical results are compared to the experimental ones (Gavanski et al. 2016; Platiša et al. 1975; Blagojević et al. 1999). As it is said before, we see that the modified semi empirical results overestimate all the experimental values, but the simplified modified semi empirical ones underestimate the experimental ones. Our quantum and the semi classical results of Griem (1974) agree well with the three measurements.

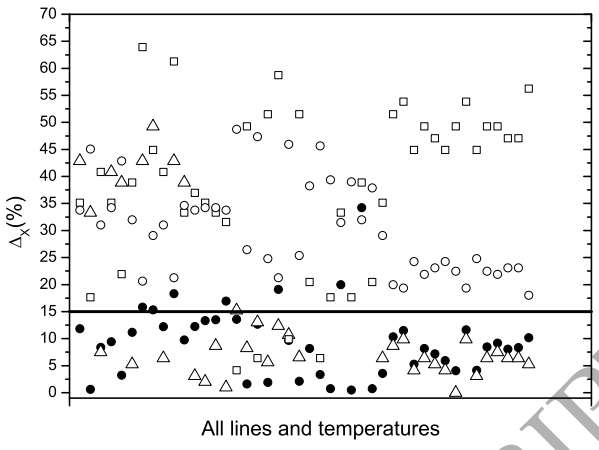

Figure 1. Relative errors Δ_X as defined in Table 1 of some O II lines between the experimental results w_m and the quantum Δ_Q (present calculations): •, the semi classical Δ_{Gr} (Griem 1974): △, the modified semi empirical $\Delta_{G(MSE)}$ (Gavanski et al. 2016): □ and the simplified modified semi empirical ones $\Delta_{G(SMSE)}$ (Gavanski et al. 2016): ○. The experimental results are those indicated in Table 1

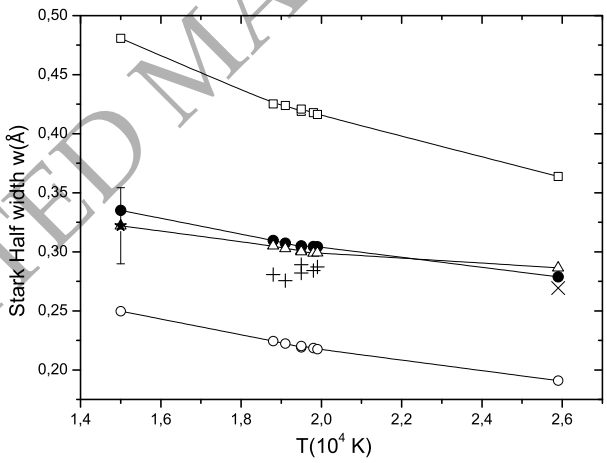

Figure 2. Stark HWHM w in Å of the O II $2p^2(^3P)3s\ ^2P_{3/2}-2p^2(^3P)3p\ ^2D^\circ_{5/2}$ line as a function of temperature at an electron density 10^{17} cm^{-3}. The experimental results of Gavanski et al. (2016): ⋆, Platiša et al. (1975): × and Blagojević et al. (1999): + are compared to the present quantum: •, to the semi classical (Griem 1974): △ (Gr), to the modified semi empirical: □ G(MSE) and to the simplified modified semi empirical ones: ○ G(SMSE). The G(MSE) and G(SMSE) results are evaluated in Gavanski et al. (2016).

3.2 Results for O III

The O III ion is studied using the five electronic configurations: $1s^2(2s^22p^2, 3s2p^3, 2s^22p3s, 2s^22p3p, 2s^22p3d)$ giving 41 fine structure levels. The scaling parameters are λ_s = 1.3630,λ_p = 1.2464 and λ_s = 1.3582. We have calculated the Stark HWHM of 20 O III lines belonging to the two transition arrays 3s−3p and 3p−3d. In Table 2, we present our quantum Stark widths for a first set of seven O III lines together with the results of the semi classical perturbation (SCP) calculations (Srećković et al. 2001b; Dimitrijević et al. 2011) and the modified semi empirical (Dimitrijević 1988) D(MSE) results. The above theoretical results are compared to the experimental ones (Blagojević et al. 2000; Srećković et al. 2001b; Platiša et al. 1975). Table 3 displays Stark widths for a second set of 13 O III lines compared to the experimental results of Srećković et al. (2005, 2001b). The measurements of Srećković et al. (2005) have been performed for one temperature value 4.2×10^4 K and those of Srećković et al. (2001b) for 5.4×10^4 K. We normalized their Stark widths to electron density N_e = 10^{17} cm^{-3}. Our quantum results are very close to the newer measurements of Srećković et al. (2005): the average error Δ_Q is about 17 per cent. The errors of the two lines $2p(^2P^o)3s\ ^3P^o_1-2p(^2P^o)3p\ ^3P_{2;1}$ are exceptionally higher than the others which lie within the experimental error bar. If we eliminate them from the

Table 1. Stark half widths at half intensity maximum (HWHM) w_Q of the O II lines. Present quantum results are compared to several experimental results w_m: *a*: Del Val et al. (1999), *b*: Djeniže et al. (1998), *c*: Platiša et al. (1975), *d*: Purić et al. (1988), *e*: Blagojević et al. (1999), *f*: Srećković et al. (2001a), *g*: Djeniže et al. (1991), and $*$ corresponds to the recent experiments of Gavanski et al. (2016). We compare also the experimental values to the semi classical results (Gr) of Griem (1974), to the modified semi empirical results G(MSE) and to the simplified modified semi empirical results G(SMSE) evaluated in Gavanski et al. (2016). w are given in Å and $\Delta_X = \frac{|w_X - w_m|}{w_m}$ is the relative difference -in per cent- between the theoretical value X and the measured one.

Transition	$T(10^4$ K)	$N_e(10^{17}$ cm$^{-3})$	w_Q	w_m	Δ_Q	Δ_{Gr}	$\Delta_{G(MSE)}$	$\Delta_{G(SMSE)}$
$2p^2(^3P)3s\ ^4P_{1/2}-2p^2(^3P)3p\ ^4D^\circ_{3/2}$	4.00	1.00	0.246	0.220[a]	12	43	35	34
$\lambda = 463.886$ nm	5.40	2.80	0.644	0.64[b]	0.63	33	18	45
	1.50	1.45	0.459	0.501*	8.4	7.5	41	31
$2p^2(^3P)3s\ ^4P_{3/2}-2p^2(^3P)3p\ ^4D^\circ_{5/2}$	4.00	1.00	0.244	0.223[a]	9.4	41	35	34
$\lambda = 464.181$ nm	5.40	2.80	0.640	0.62[b]	3.2	39	22	43
	1.50	1.45	0.453	0.510*	11	5.3	39	32
$2p^2(^3P)3s\ ^4P_{5/2}-2p^2(^3P)3p\ ^4D^\circ_{7/2}$	2.59	0.52	0.139	0.12[c]	16	43	64	21
$\lambda = 464.913$ nm	5.40	1.00	0.241	0.209[a]	15	49	45	29
	1.50	1.45	0.445	0.507*	12	9.4	41	31
$2p^2(^3P)3s\ ^4P_{1/2}-2p^2(^3P)3p\ ^4D^\circ_{1/2}$	2.59	0.52	0.142	0.12[c]	18	43	61	21
$\lambda = 465.084$ nm	4.00	1.00	0.247	0.225[a]	9.8	39	33	35
	1.50	1.45	0.459	0.523*	12	3.1	37	34
$2p^2(^3P)3s\ ^4P_{3/2}-2p^2(^3P)3p\ ^4D^\circ_{3/2}$	1.50	1.45	0.461	0.532*	13	2.0	35	34
$\lambda = 466.163$ nm								
$2p^2(^3P)3s\ ^4P_{3/2}-2p^2(^3P)3p\ ^4D^\circ_{1/2}$	1.50	1.45	0.467	0.540*	14	8.7	33	34
$\lambda = 467.373$ nm								
$2p^2(^3P)3s\ ^4P_{5/2}-2p^2(^3P)3p\ ^4D^\circ_{5/2}$	1.50	1.45	0.456	0.549*	17	0.99	32	34
$\lambda = 467.624$ nm								
$2p^2(^3P)3s\ ^4P_{3/2}-2p^2(^3P)3p\ ^4P^\circ_{1/2}$	4.00	1.00	0.223	0.258[a]	14	15	4.2	49
$\lambda = 434.556$ nm	1.50	1.45	0.435	0.428*	1.6	8.3	49	26
$2p^2(^3P)3s\ ^4P_{5/2}-2p^2(^3P)3p\ ^4P^\circ_{5/2}$	4.00	1.00	0.221	0.253[a]	13	13	6.4	47
$\lambda = 434.943$ nm	1.50	1.45	0.428	0.420*	1.9	5.7	52	25
$2p^2(^3P)3s\ ^4P_{5/2}-2p^2(^3P)3p\ ^4P^\circ_{3/2}$	2.59	0.52	0.131	0.11[c]	19	12	59	21
$\lambda = 436.689$ nm	4.00	1.00	0.224	0.248[a]	9.7	11	9.9	46
	1.50	1.45	0.435	0.426*	2.1	6.5	52	25
$2p^2(^3P)3s\ ^4P_{1/2}-2p^2(^3P)3p\ ^4S^\circ_{3/2}$	2.59	0.52	0.119	0.11[c]	8.2	–	20	38
$\lambda = 371.274$ nm	4.34	1.59	0.306	0.296[d]	3.4	–	6.4	46
	1.50	1.45	0.408	0.411*	0.73	–	18	39
$2p^2(^3P)3s\ ^4P_{3/2}-2p^2(^3P)3p\ ^4S^\circ_{3/2}$	2.59	0.52	0.120	0.10[c]	20	–	33	32
$\lambda = 372.732$ nm	1.50	1.45	0.410	0.412*	0.49	–	18	39
$2p^2(^3P)3s\ ^4P_{5/2}-2p^2(^3P)3p\ ^4S^\circ_{3/2}$	5.40	2.80	0.510	0.38[b]	34	–	39	32
$\lambda = 374.949$ nm	1.50	1.45	0.412	0.409*	0.73	–	20	38
$2p^2(^3P)3s\ ^2P_{3/2}-2p^2(^3P)3p\ ^2D^\circ_{5/2}$	2.59	0.52	0.145	0.14[c]	3.6	6.4	35	29
$\lambda = 441.491$ nm	1.88	0.31	0.096	0.087[e]	10	8.7	52	20
	1.91	0.41	0.126	0.113[e]	12	9.9	54	19
	1.95	0.46	0.140	0.133[e]	5.3	4.2	45	24
	1.95	0.39	0.119	0.110[e]	8.2	6.4	49	22
	1.98	0.44	0.134	0.125[e]	7.2	5.3	47	23
	1.99	0.47	0.143	0.135[e]	5.9	4.2	45	24
	1.50	1.45	0.486	0.467*	4.1	0.0	49	22
$2p^2(^3P)3s\ ^2P_{1/2}-2p^2(^3P)3p\ ^2D^\circ_{3/2}$	1.88	0.31	0.096	0.086[e]	12	9.9	54	19
$\lambda = 441.697$ nm	1.91	0.41	0.126	0.121[e]	4.1	3.1	45	25
	1.95	0.46	0.141	0.130[e]	8.5	6.4	49	22
	1.95	0.39	0.119	0.109[e]	9.2	7.5	49	22
	1.98	0.44	0.134	0.124[e]	8.1	6.4	47	23
	1.99	0.47	0.143	0.132[e]	8.3	6.4	47	23
	1.50	1.45	0.487	0.442*	10	5.3	56	18

Table 1. *continued.*

Transition	$T(10^4$ K)	$N_e(10^{17}$ cm$^{-3})$	w_Q	w_m	Δ_Q	Δ_{Gr}	$\Delta_{G(MSE)}$	$\Delta_{G(SMSE)}$
$2p^2(^3P)3s\ ^2P_{1/2}-2p^2(^3P)3p\ ^2P^\circ_{3/2}$	1.20	0.76	0.241	0.252^f	4.4	19	33	29
$\lambda = 394.504$ nm	1.38	0.91	0.274	0.358^f	23	34	4.2	44
	1.57	1.45	0.415	0.349^f	19	3.1	61	15
	1.83	1.82	0.492	0.546^f	9.9	21	19	36
	2.03	1.25	0.325	0.464^f	30	38	9.1	51
	1.50	1.45	0.422	0.367^*	15	0.0	56	17
$2p^2(^3P)3s\ ^2P_{1/2}-2p^2(^3P)3p\ ^2P^\circ_{1/2}$	5.40	2.80	0.535	0.54^b	0.93	3.1	20	42
$\lambda = 395.436$ nm	1.20	0.76	0.242	0.288^f	16	29	16	38
	1.38	0.91	0.275	0.312^f	12	24	20	35
	1.57	1.45	0.416	0.495^f	16	26	14	39
	1.83	1.82	0.494	0.477^f	3.6	8.3	37	27
	2.03	1.25	0.327	0.278^f	18	5.3	52	18
	1.50	1.45	0.424	0.368^*	15	0.0	56	17
$2p^2(^3P)3s\ ^2P_{3/2}-2p^2(^3P)3p\ ^2P^\circ_{3/2}$	2.59	0.52	0.126	0.12^c	5.0	2.0	32	29
$\lambda = 397.326$ nm	1.50	1.45	0.428	0.415^*	3.1	11	39	25
$2p^2(^3P)3s\ ^2P_{3/2}-2p^2(^3P)3p\ ^2P^\circ_{1/2}$	1.50	1.45	0.430	0.412^*	4.1	11	41	18
$\lambda = 398.271$ nm								
$2p^2(^3P)3p\ ^4D^\circ_{5/2}-2p^2(^3P)3d\ ^4F_{7/2}$	2.59	0.52	0.106	0.12^c	12	16	35	46
$\lambda = 407.216$ nm	4.00	1.00	0.176	0.239^a	26	7.5	4.2	58
	1.20	0.76	0.209	0.373^f	44	36	7.4	63
	1.38	0.91	0.236	0.425^f	44	35	9.1	63
	1.57	1.45	0.357	0.554^f	36	22	4.2	58
	1.83	1.82	0.422	0.568^f	26	8.3	18	52
	2.05	0.98	0.218	0.310^f	30	12	9.9	56
	1.50	1.45	0.364	0.480^*	24	9.9	23	32
$2p^2(^3P)3p\ ^4D^\circ_{5/2}-2p^2(^3P)3d\ ^4F_{5/2}$	4.00	1.00	0.179	0.252^a	29	2.0	0.0	60
$\lambda = 408.511$ nm	1.20	0.76	0.212	0.284^f	25	15	22	51
	1.38	0.91	0.239	0.293^f	18	5.7	33	47
	1.57	1.45	0.362	0.370^f	2.2	16	56	12
	1.83	1.82	0.428	0.520^f	18	1.0	30	48
	2.05	0.98	0.221	0.295^f	25	6.5	16	53
	1.50	1.45	0.369	0.492^*	25	–	20	51
$2p^2(^1D)3s\ ^2D_{5/2}-2p^2(^1D)3p\ ^2F^\circ_{7/2}$	2.59	0.52	0.142	0.13^c	9.2	–	52	25
$\lambda = 459.097$ nm	4.00	1.00	0.244	0.223^a	9.4	–	37	32
	1.50	1.45	0.461	0.385^*	20	–	85	7.4
$2p^2(^1D)3s\ ^2D_{3/2}-2p^2(^1D)3p\ ^2F^\circ_{5/2}$	2.59	0.52	0.143	0.13^c	10	–	52	25
$\lambda = 459.618$ nm	4.00	1.00	0.246	0.272^a	9.6	–	12	44
	5.40	2.80	0.641	0.42^b	53	–	82	13
	1.50	1.45	0.465	0.398^*	17	–	82	9.1
$2p^2(^1D)3s\ ^2D_{3/2}-2p^2(^1D)3p\ ^2P^\circ_{1/2}$	1.50	1.45	0.468	0.358^*	31	–	54	24
$\lambda = 391.929$ nm 24 – 53								
$2p^2(^3P)3p\ ^4P^\circ_{3/2}-2p^2(^3P)3d\ ^4P_{5/2}$	2.59	0.52	0.115	0.13^c	12	11	33	43
$\lambda = 415.330$ nm	4.00	1.00	0.190	0.293^a	35	12	8.3	61
	1.50	1.45	0.396	0.540^*	27	16	18	49
$2p^2(^3P)3p\ ^4P^\circ_{5/2}-2p^2(^3P)3d\ ^4P_{5/2}$	1.50	1.45	0.398	0.545^*	27	16	18	49
$\lambda = 416.923$ nm								
$2p^2(^3P)3p\ ^2D^\circ_{3/2}-2p^2(^3P)3d\ ^4D_{5/2}$	6.00	0.81	0.180	0.240^g	25	–	5.3	56
$\lambda = 471.001$ nm $T12 - T19$	1.50	1.45	0.512	0.686^*	25	–	25	44
$2p^2(^3P)3p\ ^2D^\circ_{5/2}-2p^2(^3P)3d\ ^2F_{7/2}$	1.88	0.31	0.106	0.115^e	7.8	9.9	45	36
$\lambda = 470.535$ nm	1.91	0.41	0.140	0.170^e	18	2.0	28	44
	1.95	0.46	0.156	0.195^e	20	3.8	23	45
	1.95	0.39	0.132	0.146^e	9.6	8.7	41	38
	1.98	0.44	0.148	0.174^e	15	2.0	32	42
	1.99	0.47	0.158	0.189^e	16	1.0	30	43
	6.00	0.70	0.159	0.240^e	34	7.5	7.4	61
	1.50	1.45	0.544	0.624^*	13	0.0	39	39
$2p^2(^3P)3p\ ^2D^\circ_{3/2}-2p^2(^3P)3d\ ^2D_{5/2}$	6.00	0.70	0.165	0.254^g	35	–	9.9	60
$\lambda = 435.939$ nm	1.50	1.45	0.494	0.583^*	15	–	32	38
$2p^2(^3P)3p\ ^4S^\circ_{3/2}-2p^2(^3P)3d\ ^4P_{1/2}$	5.40	2.80	0.715	0.94^b	24	23	5.3	55
$\lambda = 489.086$ nm	1.50	1.45	0.571	0.751^*	24	8.3	23	45
$2p^2(^3P)3p\ ^4S^\circ_{3/2}-2p^2(^3P)3d\ ^4P_{5/2}$	6.00	0.81	0.201	0.232^g	13	47	22	50
$\lambda = 492.453$ nm	1.50	1.45	0.576	0.762^*	24	8.3	23	45

comparison, the average relative error becomes 8 per cent. This is not the case for the old measurements of Blagojević et al. (2000), where the relative error is about 48 per cent. Contrarily to our quantum results, the D(MSE) ones are closer to the experimental results of Blagojević et al. (2000) ($\Delta_{\rm MSE}$ = 20 per cent), while they present a difference of 44 per cent with Srećković et al. (2005) results. The Stark widths evaluated by the semi classical perturbation method (SCP) are measured only in Blagojević et al. (2000), and they agree with them within 30 per cent. We notice that the two experimental procedures considered here are different, especially in the methods used for determining the electron density. Figure 3 shows an illustration of the behaviour of Stark half width at half intensity maximum with temperature for the two O III lines $2p(^2P^o)3s\ ^3P^o_1 - 2p(^2P^o)3p\ ^3D_2$ and $2p(^2P^o)3p\ ^3S_1 - 2p(^2P^o)3d\ ^3P^o_0$. For the considered lines and for all the temperature values, our results are higher than all the others, but we see from Figure 3 that the agreement between the quantum, the D(MSE) and the SCP results can change with the temperature. This behaviour is maybe due to the effects of strong collisions and resonances which are important at low temperatures, and they are differently taken into account in the three approaches. This point will be discussed in details in subsection 3.5.

3.3 Results for Si II

We use in our structure and collision study for the singly ionized silicon the 10 following electronic configurations: $1s^22s^22p^6$ ($3s^23p$, $3s3p^2$, $3s^24s$, $3s^23d$, $3s^24p$, $3s^25s$, $3s^24d$, $3s^24f$, $3s3p3d$, $3s3p4p$) giving rise to 61 fine structure levels. The scaling parameters λ_l provided by the code SSTRUCTURE are λ_s = 1.1054, λ_p = 1.0274, λ_d = 1.1464, and λ_f = 1.2569. We calculate the Stark broadening of 9 spectral lines. Our quantum Stark HWHM and the available theoretical ones: semi classical (Griem 1974), results of Gavanski et al. (2016) obtained by using the modified semi empirical theory of Dimitrijević & Konjević (1980) and its simplified form of Dimitrijević & Konjević (1987) are compared to the experimental results of: Konjević et al. (1970); Purić et al. (1973); Lesage & Miller (1975); Lesage et al. (1977, 1983); Lesage & Redon (2004); Chiang & Griem (1978); Pérez et al. (1990, 1993); Wollschläger et al. (1997); González et al. (2002); Bukvić et al. (2009), and the recent experiments of Gavanski et al. (2016).

Table 4 displays our Stark HWHM w_Q, the semi classical $w_{\rm Gr}$ (Griem 1974), the modified semi empirical $w_{\rm G(MSE)}$ and the simplified modified semi empirical $w_{\rm G(SMSE)}$ ones compared to the experimental results w_m of the 9 Si II lines for different temperatures and densities. The G(MSE) and the G(SMSE) calculations are performed in Gavanski et al. (2016). The first part of the Table 4, where the lines arising from the transition array $3s3p^2 - 3s^24p$ are displayed, shows that the relative error Δ_Q between the quantum and the experimental results is about 19 per cent, that of the simplified modified semi empirical results $\Delta_{\rm G(SMSE)}$ is about 34 per cent. The second part of Table 4 contains Stark widths of lines arising from the transition arrays 4s−4p, 3d−4f and 4p−4d. The average relative error becomes higher: 32 per cent for the quantum results and 46 per cent for the G(SMSE) ones. The average relative error for the semi classical results of Griem (1974) is about 40 per cent, and that of the modified semi empirical results is about 30 per cent. In conclusion, our quantum Stark widths are the most close to the experimental results (nearly 25 per cent for all the lines). The experimental results of Konjević et al. (1970) and Purić et al. (1973) present the higher disagreement with our quantum calculations and the semi classical ones. We remark also that -in almost all the cases- these experimental Stark widths are underestimated compared to our quantum ones, but agree with the simplified modified semi empirical results G(SMSE).

Figure 4 displays the relative difference Δ_X between the experimental results and the theoretical ones (including our quantum results) for the 9 Si II lines displayed in Table 4. We see that about 70 per cent of our quantum results agree with the experimental ones within 0 − 20 per cent. For the relative errors of the simplified modified semi empirical results (Gavanski et al. 2016), only 16 percent of them agree with the experimental ones within 0 − 20 per cent. The results in the Figure 4 are averaged over all the Si II lines and the temperature values.

As an illustration, we display in Figure 5 the Stark HWHM w of the Si II $3s^24s\ ^2S_{1/2} - 3s^24p\ ^2P^o{}_{1/2}$ line. We can see an acceptable agreement between our quantum results and those obtained by Gavanski et al. (2016) using the modified semi empirical method of Dimitrijević & Konjević (1980). The experimental results of Konjević et al. (1970) and Purić et al. (1973) present the higher disagreement with our quantum calculations. We remark also that -in almost all the cases- these experimental Stark widths are underestimated compared to our quantum ones. In these cases, the G(SMSE) results of Gavanski et al. (2016) obtained using the simplified modified semi empirical method of Dimitrijević & Konjević (1987) are in acceptable agreement with the results of Konjević et al. (1970) and Purić et al. (1973). The same disagreement is also detected between the same experimental results of Konjević et al. (1970) and Purić et al. (1973) and the semi classical and the modified semi empirical calculations.

3.4 Results for Si III

We use in our structure and collision study for the Si III ion the 13 following electronic configurations: $1s^22s^22p^6$ ($3s^2$, $3s3p$, $3p^2$, $3s3d$, $3s4s$, $3s4p$, $3s4d$, $3s4f$, $3s5s$, $3s5p$, $3s5d$, $3s5f$, $3s5g$). This set of configurations gives rise to 46 fine structure levels. The scaling parameters λ_l are λ_s = 1.1028, λ_p = 1.0176, λ_d = 1.0035, λ_f = 1.1862 and λ_g = 1.297. Using our quantum method, we calculated the Stark widths $w_{\rm Q}$ of 12 Si III spectral lines, and we report them in Table 5 together with the results of Gavanski et al. (2016) obtained by using the modified semi emiprical theory (MSE) of Dimitrijević & Konjević (1980) and its simplified form (SMSE) of Dimitrijević & Konjević (1987). The results of Gavanski et al. (2016) will be denoted as G(MSE) and G(SMSE). The three theoretical Stark widths ($w_{\rm Q}$, $w_{\rm G(MSE)}$, and $w_{\rm G(SMSE)}$) are compared to the experimental results of Bukvić et al. (2009); Djeniže et al. (1992); Purić et al. (1974); Platiša et al. (1977); González et al. (2002); Kusch & Schroeder (1982), and Gavanski et al. (2016). Table 5 displays also the relative errors Δ_X between the theoretical and the experimental results. The average relative error for our quantum calculations is $\Delta_{\rm Q}$ = 22 per cent, that of the G(MSE) results is $\Delta_{\rm G(MSE)}$ = 27 per cent and that of the G(SMSE) is $\Delta_{\rm G(SMSE)}$ = 35 per cent. The high disagreement has been detected for the 3s4f $^1F^o{}_3 - 3s5g\ ^1G_4$ line: $\Delta_{\rm Q}$ = 31, $\Delta_{\rm G(MSE)}$ = 48, and $\Delta_{\rm G(SMSE)}$ = 58 per cent. We remark that the relative difference between our quantum results and the recent experiments of Gavanski et al. (2016) is very good for the transitions 3d−4p and 4s−4p (about 5 per cent). However, it is about 28 per cent for the 4p−4d transitions. We remark also that the higher disagreement corresponds to the two "older" experiments of Purić et al. (1974) (c) and Platiša et al. (1977) (d). This disagreement is also found for all the theoretical results presented in the Table 5.

Figure 6 displays the relative difference Δ_X between the ex-

Table 2. Quantum Stark HWHM (in Å) for some O III lines: our quantum results w_Q, the modified semi empirical results $w_{\mathrm{D(MSE)}}$ (Dimitrijević 1988) and the semi classical perturbation w_{SCP} calculations (Srećković et al. 2001b; Dimitrijević et al. 2011) are compared to the experimental results w_m of Blagojević et al. (2000). Other experiments: Srećković et al. (2005) (*a*) and Srećković et al. (2001b) (*b*). Δ_X is defined in Table 1.

Transition	$T(10^4$ K)	$N_e(10^{17}$ cm$^{-3})$	w_Q	w_m	$w_{\mathrm{D(MSE)}}$	w_{SCP}	Δ_Q	$\Delta_{\mathrm{D(MSE)}}$	Δ_{SCP}
$2p(^2P^o)3p\ ^3D_2-2p(^2P^o)3d\ ^3F^o_3$	1	1	0.1603	–	0.0980	–			
$\lambda = 326.098$ nm	2	1	0.1179	–	0.0630	–			
	2.6	0.32	0.0337	0.0235	0.0188	–	43	20	
	3.97	0.83	0.0734	0.0500	0.0391	–	47	22	
	4	1	0.0882	–	0.0446	–			
	8	1	0.0671	–	0.0334	–			
$2p(^2P^o)3p\ ^3D_3-2p(^2P^o)3d\ ^3F^o_4$	1	1	0.1557	–		–			
$\lambda = 326.546$ nm	2	1	0.1146	–		–			
	2.6	0.32	0.0328	0.0225		–	46	16	
	3.34	0.64	0.0592	0.0405	0.0326	–	46	20	
	3.97	0.83	0.0715	0.0500		–	43	22	
	4	1	0.0859	–		–			
	4.6	1.05	0.0654	0.0670	0.0443	–	2	34	
$2p(^2P^o)3p\ ^3D_1-2p(^2P^o)3d\ ^3F^o_2$	1	1	0.1599	–		–			
$\lambda = 326.731$ nm	2	1	0.1176	–		–			
	3.97	0.83	0.0734	0.0515		–	43	24	
	4	1	0.0881	–		–			
	8	1	0.0672	–		–			
$2p(^2P^o)3p\ ^3D_2-2p(^2P^o)3d\ ^3F^o_2$	1	1	0.1636	–	–	–			
$\lambda = 328.183$ nm	2	1	0.1202	–	–	–			
	4	1	0.0900	–	–	–			
	4.2	1.65	0.1455	0.09(15)[a]	–	–	62		
	8	1	0.0685	–	–	–			
$2p(^2P^o)3p\ ^3D_3-2p(^2P^o)3d\ ^3F^o_3$	1	1	0.1612	–	–	–			
$\lambda = 328.445$ nm	2	1	0.1185	–	–	–			
	4	1	0.0887	–	–	–			
	4.2	1.65	0.1435	0.120(17)[a]	–	–	20		
$2p(^2P^o)3s\ ^3P^o_1-2p(^2P^o)3p\ ^3D_2$	1	1	0.2018	–	0.1150	0.1730			
$\lambda = 375.467$ nm	1.83	0.33	0.0557	0.0375	0.0286	0.0456	49	24	22
	1.91	0.41	0.0683	0.0405	0.0352	0.0554	69	13	3
	1.95	0.46	0.0761	0.0520	0.0393	0.0616	46	24	18
	1.99	0.47	0.0773	0.0455	0.0400	0.0625	70	12	37
	2	1	0.1642	–	0.0815	0.1230			
	2.59	0.52	0.0790	0.0380[b]		0.0617	108		62
	4	1	0.1332	–	0.0575	0.0975			
	5.4	2.8	0.3408	0.1900[b]		0.2366	79		25
	10	1	0.1008	–	0.0398	0.0630			
$2p(^2P^o)3s\ ^3P^o_2-2p(^2P^o)3p\ ^3D_3$	1	1	0.1961	–					
$\lambda = 375.988$ nm	1.83	0.33	0.0546	0.0335			63	15	36
	1.91	0.41	0.0670	0.0415			61	15	33
	1.95	0.46	0.0747	0.0485			54	19	27
	1.99	0.47	0.0759	0.0490			55	18	28
	2	1	0.1612	–					
	4	1	0.1315	–					
	5.4	2.8	0.3369	0.2000[b]		0.2366	68		18
	10	1	0.0998	–					

perimental results and the theoretical ones (including our quantum results) for the 12 Si III lines displayed in Table 5. The results are averaged over all the temperatures and over all the lines. We see that 65 per cent of our quantum results collected in Figure 6 agree with relative error less than 30 per cent with the experimental ones.

As an illustration of the behaviour of calculated and measured Stark widths with electron temperature, we display in Figure 7, the HWHM w of the two Si III lines: $3s4f\ ^1F^\circ_3-3s5g\ ^1G_4$ (left panel) and $3s3d\ ^3D_1-3s4p\ ^3P^\circ_0$ (right panel). The comparisons have been done with the experimental works of Djeniže et al. (1992), Bukvić et al. (2009) and Gavanski et al. (2016). We have chosen these two lines to show how widespread the results are, and to show that the behaviour of the theoretical results versus the measured ones is different from a line to another. We can see that the results of the line $3s4f\ ^1F^\circ_3-3s5g\ ^1G_4$ are very dispersed, while the measured and calculated widths of the line $3s3d\ ^3D_1-3s4p\ ^3P^\circ_0$ are almost in agreement within 15 per cent, except the experimental result of Bukvić et al. (2009) which is slightly different from all the other results. The observed dispersion of the available results (measured and calculated) represents an obstacle to make a decision about their accuracy, but we see clearly that in average, our quantum results are the most close to the experimental ones.

Table 3. Same as in Table 2 but for other O III lines compared to the experimental results of Srećković et al. (2005) (*a*) and to those of Srećković et al. (2001b) (*b*). Values are normalized to $N_e = 10^{17}$ cm^{-3}. D(MSE) results are from Dimitrijević (1988) and the SCP ones are from Srećković et al. (2001b); Dimitrijević et al. (2011).

Transition	$T(10^4$ K)	w_Q	w_m	$w_{\mathrm{D(MSE)}}$	w_{SCP}	Δ_Q	$\Delta_{\mathrm{D(MSE)}}$
$2p(^2P^o)3p\ ^1P_1-2p(^2P^o)3d\ ^1D^o_2$	1	0.1488	–	–	–		
$\lambda = 295.69$ nm	2	0.1075	–	–	–		
	4	0.0789	–	–	–		
	4.2	0.0772	0.0788(12)^a	–	–	2	
	8	0.0587	–	–	–		
$2p(^2P^o)3p\ ^3D_1-2p(^2P^o)3d\ ^3D^o_1$	1	0.1459	–	–	–		
$\lambda = 299.648$ nm	2	0.1061	–	–	–		
	4	0.0788	–	–	–		
	4.2	0.0772	0.0727(15)^a	–	–	6	
	8	0.0595	–	–	–		
$2p(^2P^o)3p\ ^3D_2-2p(^2P^o)3d\ ^3D^o_3$	1	0.1444	–	–	–		
$\lambda = 299.769$ nm	2	0.1050	–	–	–		
	4	0.0779	–	–	–		
	4.2	0.0764	0.0606(15)^a	–	–	26	
$2p(^2P^o)3s\ ^3P^o_1-2p(^2P^o)3p\ ^3P_2$	1	0.1792	–	0.0790	–		
$\lambda = 302.342$ nm	2	0.1317	–	0.0560	–		
	4	0.0994	–	0.0396	–		
	4.2	0.0975	0.0697(12)^a	0.0657	–	40	43
	8	0.0767	–	0.0300	–		
$2p(^2P^o)3s\ ^3P^o_1-2p(^2P^o)3p\ ^3P_1$	1	0.1811	–		–		
$\lambda = 303.541$ nm	2	0.1330	–		–		
	4	0.1004	–		–		
	4.2	0.0985	0.0697(12)^a		–	41	43
$2p(^2P^o)3p\ ^3S_1-2p(^2P^o)3d\ ^3P^o_0$	1	0.1497	–	0.0855	–		
$\lambda = 311.567$ nm	2	0.1090	–	0.0605	–		
	4	0.0812	–	0.0427	–		
	4.2	0.0796	0.0727(10)^a	0.0709	–	9	41
	8	0.0618	–	0.0313	–		
$2p(^2P^o)3p\ ^3S_1-2p(^2P^o)3d\ ^3P^o_1$	1	0.1499	–		–		
$\lambda = 312.163$ nm	2	0.1092	–		–		
	4	0.0813	–		–		
	4.2	0.0797	0.0848(10)^a		–	6	49
$2p(^2P^o)3p\ ^3S_1-2p(^2P^o)3d\ ^3P^o_2$	1	0.1502	–		–		
$\lambda = 313.279$ nm	2	0.1094	–		–		
	4	0.0815	–		–		
	4.2	0.0799	0.0788(10)^a		–	1	45
$2p(^2P^o)3s\ ^3P^o_0-2p(^2P^o)3p\ ^3S_1$	1	0.1684	–	0.0924	0.1360		
$\lambda = 329.939$ nm	2	0.1328	–	0.0655	0.0965		
	4	0.1051	–	0.0463	0.0767		
	8	0.0841	–	0.0349	0.0556		
	10	0.0783	–	0.0331	0.0495		
$2p(^2P^o)3s\ ^3P^o_1-2p(^2P^o)3p\ ^3S_1$	1	0.1691	–				
$\lambda = 331.233$ nm	2	0.1335	–				
	4	0.1057	–				
	8	0.0845	–				
	10	0.0787	–				
$2p(^2P^o)3s\ ^3P^o_2-2p(^2P^o)3p\ ^3S_1$	1	0.1710	–				
$\lambda = 334.077$ nm	2	0.1351	–				
	4	0.1070	–				
	5.4	0.0971	0.0464^b		0.0627	109	35
	8	0.0857	–				
	10	0.0798	–				
$2p(^2P^o)3p\ ^3P_1-2p(^2P^o)3d\ ^3D^o_2$	1	0.2164	–	0.1230			
$\lambda = 370.727$ nm	2	0.1587	–	0.0865			
	4	0.1187	–	0.0610			
	4.2	0.1164	0.1061(10)^a	0.1031		10	41
	8	0.0903	–	0.0454			
$2p(^2P^o)3p\ ^3P_2-2p(^2P^o)3d\ ^3D^o_2$	1	0.2183	–				
$\lambda = 372.531$ nm	2	0.1602	–				
	4	0.1198	–				
	4.2	0.1175	0.1152(10)^a			2	46

Table 4. Present quantum Stark HWHM w_Q of the Si II lines compared to different experimental results w_m: *a*: Wollschläger et al. (1997), *b*: González et al. (2002), *c*: Bukvić et al. (2009), *d*: Konjević et al. (1970), *e*: Purić et al. (1973), *f*: Lesage et al. (1977), *g*: Chiang & Griem (1978), *h*: Lesage et al. (1983), *i*: Pérez et al. (1990), *j*: Pérez et al. (1993), *k*: Lesage & Miller (1975), *l*: Lesage & Redon (2004), and * corresponds to the recent experiments of Gavanski et al. (2016). We compare also w_m to the semi classical results (Gr) of Griem (1974), to the modified semi empirical results G(MSE) and to the simplified modified semi empirical results G(SMSE) performed in Gavanski et al. (2016). Results are given in Å and $\Delta_X = \frac{|w_X - w_m|}{w_m}$ is the relative difference -in per cent- between the theoretical value X and the measured one.

Transition	$T(10^4$ K)	$N_e(10^{17}$ cm$^{-3})$	w_Q	w_m	Δ_Q	Δ_{Gr}	$\Delta_{G(MSE)}$	$\Delta_{G(SMSE)}$
$3s3p^2\ ^2D_{3/2}-3s^24p\ ^2P^\circ_{3/2}$	1.20	1.00	0.610	0.57[a]	7.0			33
λ = 385.366 nm	1.21		0.608	0.54[a]	13			29
	1.25		0.599	0.55[a]	8.9			32
	1.34		0.580	0.57[a]	1.8			36
	1.80	1.00	0.508	0.52[b]	2.3			40
	1.50	1.00	0.551	0.535[c]	3.0			36
	1.50	1.45	0.799	0.631*	27			21
$3s3p^2\ ^2D_{5/2}-3s^24p\ ^2P^\circ_{3/2}$	0.85	1.00	0.709	0.40[d]	77			14
λ = 385.602 nm	0.97		0.666	0.38[d]	75			12
	0.87	1.00	0.701	0.52[e]	35			13
	1.06		0.639	0.54[e]	18			24
	1.28		0.586	0.56[e]	4.6			34
	1.64		0.524	0.56[e]	6.4			41
	1.00	1.00	0.656	1.07[f]	39			61
	1.80	1.00	0.502	1.00[g]	50			69
	1.60	1.00	0.529	0.64[h]	17			48
	2.00		0.479	0.68[h]	30			56
	2.20		0.460	0.66[h]	30			57
	1.20	1.00	0.603	0.59[a]	2.2			35
	1.21		0.601	0.51[a]	18			25
	1.25		0.592	0.50[a]	18			25
	1.26		0.590	0.60[a]	1.7			38
	1.34		0.574	0.58[a]	1.0			38
	1.35		0.572	0.58[a]	1.4			38
	1.36		0.570	0.53[a]	7.5			32
	1.40		0.562	0.60[a]	6.3			41
	1.43		0.557	0.53[a]	5.1			34
	1.43		0.557	0.51[a]	9.2			31
	1.80	1.00	0.502	0.50[b]	0.40			37
	1.50	1.00	0.545	0.490[c]	11			30
	1.50	1.45	0.790	0.669*	18			25
$3s3p^2\ ^2D_{5/2}-3s^24p\ ^2P^\circ_{1/2}$	0.85	1.00	0.724	0.42[d]	72			8.7
λ = 386.260 nm	0.97		0.681	0.42[d]	62			2.0
	0.87	1.00	0.716	0.44[e]	63			3.1
	1.06		0.653	0.48[e]	36			15
	1.28		0.599	0.50[e]	20			25
	1.64		0.535	0.48[e]	11			32
	1.00	1.00	0.671	1.05[f]	36			60
	1.80	1.00	0.513	0.98[g]	48			68
	1.60	1.00	0.541	0.64[h]	15			48
	2.00		0.490	0.68[h]	28			56
	2.20		0.470	0.66[h]	29			57
	1.20	1.00	0.617	0.63[a]	2.1			39
	1.21		0.614	0.56[a]	9.6			32
	1.25		0.605	0.60[a]	0.83			37
	1.31		0.592	0.61[a]	3.0			40
	1.34		0.586	0.53[a]	11			32
	1.35		0.584	0.57[a]	2.5			36
	1.36		0.582	0.60[a]	3.0			40
	1.40		0.575	0.53[a]	8.5			33
	1.43		0.569	0.61[a]	6.7			42
	1.43		0.569	0.51[a]	12			31
	1.80	1.00	0.513	0.50[b]	2.6			37
	1.50	1.00	0.557	0.430[c]	30			20
	1.50	1.45	0.808	0.589*	37			15

Table 4. *Continued.*

Transition	$T(10^4$ K)	$N_e(10^{17}$ cm$^{-3})$	w_Q	w_m	Δ_Q	Δ_{Gr}	$\Delta_{G(MSE)}$	$\Delta_{G(SMSE)}$
$3s^24s\ ^2S_{1/2}-3s^24p\ ^2P^\circ_{3/2}$	0.85	1.00	2.037	1.34[d]	52	82	64	23
λ = 634.710 nm	1.00	1.00	1.898	1.96[f]	3.2	19	3.1	22
	1.80	1.00	1.493	2.14[g]	30	6.5	30	47
	1.60	1.00	1.563	1.24[h]	26	67	28	2.9
	2.00		1.434	1.24[h]	16	59	15	14
	2.20		1.383	1.28[h]	8.0	49	6.4	20
	3.50	0.98	1.148	1.20[i]	4.3	45	9.9	34
	1.39	0.565	0.935	1.20[j]	22	1.0	19	39
	1.64	0.662	1.025	1.25[j]	18	8.7	17	37
	3.15	0.919	1.117	1.22[j]	8.4	35	14	35
	1.80	1.00	1.493	1.13[b]	32	79	33	0.0
	1.25	1.00	1.728	1.85[c]	6.6	19	2.0	26
	1.50	1.45	2.326	1.582*	47	92	52	14
$3s^24s\ ^2S_{1/2}-3s^24p\ ^2P^\circ_{1/2}$	0.85	1.00	2.063	1.30[d]	59	89	69	27
λ = 637.136 nm	0.87	1.00	2.042	1.00[e]	100	144	117	64
	1.06		1.875	1.04[e]	80	122	89	43
	1.28		1.733	0.92[e]	88	138	96	47
	1.64		1.568	0.82[e]	91	150	92	45
	1.00	1.00	1.923	1.93[f]	0.36	22	5.3	21
	1.80	1.00	1.512	2.22[g]	32	9.1	32	49
	1.60	1.00	1.583	1.24[h]	28	67	30	2.9
	2.00		1.452	1.10[h]	32	79	32	2.0
	2.20		1.400	1.28[h]	9.4	52	7.5	19
	3.50	0.98	1.162	1.26[i]	7.8	39	14	37
	1.39	0.565	0.947	1.22[j]	22	0.0	20	40
	1.64	0.662	1.038	1.23[j]	16	11	15	36
	3.15	0.919	1.130	1.29[j]	12	28	18	39
	1.80	1.00	1.512	0.99[b]	53	104	54	15
	1.25	1.00	1.75	1.87[c]	6.4	18	2.9	27
	1.50	1.45	2.355	1.691*	39	82	43	6.4
$3s^23d\ ^2D_{3/2}-3s^24f\ ^2F^\circ_{5/2}$	1.00	1.00	1.051	1.58[f]	33	13	32	76
λ = 412.807 nm	1.60	1.00	0.829	1.00[h]	17	27	4.8	70
	2.00		0.741	0.96[h]	23	28	5.7	72
	2.20		0.706	1.04[h]	32	16	15	76
	1.39	0.565	0.503	1.29[j]	61	43	57	86
	1.64	0.662	0.542	1.31[j]	59	36	52	85
	1.80	1.00	0.781	0.97[b]	19	28	4.8	71
	1.50	1.00	0.857	1.05[c]	18	22	8.3	71
	1.50	1.45	1.242	1.482*	16	25	5.7	70
$3s^23d\ ^2D_{5/2}-3s^24f\ ^2F^\circ_{7/2}$	1.00	1.00	1.033	1.60[f]	35	14	32	77
λ = 413.089 nm	1.60	1.00	0.815	1.00[h]	19	27	4.8	70
	2.00		0.728	0.96[h]	24	28	5.7	72
	2.20		0.693	1.04[h]	33	18	15	76
	1.39	0.565	0.494	1.43[j]	65	49	61	87
	1.64	0.662	0.533	1.47[j]	64	43	57	87
	3.15	0.919	0.530	1.91[j]	72	44	59	90
	1.80	1.00	0.768	1.01[b]	24	23	8.3	72
	1.50	1.00	0.842	1.20[c]	30	7.5	19	74
	1.50	1.45	1.220	1.487*	18	25	5.7	70
$3s^24p\ ^2P^\circ_{3/2}-3s^24d\ ^2D_{5/2}$	1.00	1.00	2.172	3.5[k]	38	18	40	51
λ = 505.598 nm	1.00	1.00	2.172	2.69[f]	19	27	22	37
	1.60	1.00	1.712	2.00[h]	14	37	7.4	33
	2.00		1.528	2.40[h]	36	12	26	50
	2.20		1.456	2.12[h]	31	27	17	46
	3.50	0.98	1.127	2.01[i]	44	27	20	56
	1.39	0.565	1.039	1.80[j]	42	13	40	55
	1.64	0.662	1.119	2.04[i]	45	11	40	57
	3.15	0.919	1.115	2.08[i]	46	16	26	58
	1.80	1.00	1.612	2.58[b]	38	5.3	30	51
	1.50	1.00	1.769	2.50[c]	29	9.9	25	44
	1.50	1.45	2.564	2.93*	12	37	6.5	32
$3s3p(^3P^\circ)3d\ ^4F^\circ_{9/2}-3s3p(^3P^\circ)4p\ ^4D_{7/2}$	1.80	1.00	0.473	0.67[b]	29	–	23	37
λ = 566.956 nm	1.50	1.45	0.742	0.943*	21	–	41	29

Table 5. Present quantum Stark HWHM w_Q of the Si III lines compared to different experimental results w_m: *a*: Bukvić et al. (2009), *b*: Djeniže et al. (1992), *c*: Purić et al. (1974), *d*: Platiša et al. (1977), *e*: González et al. (2002), *f*: Kusch & Schroeder (1982), and * corresponds to the recent experiments of Gavanski et al. (2016). We compare also the experimental values to the G(MSE) results obtained in Gavanski et al. (2016) using the modified semi empirical approach (Dimitrijević & Konjević 1980) and to the G(SMSE) results obtained in Gavanski et al. (2016) using the simplified modified semi empirical approach (Dimitrijević & Konjević 1987). Results are given in Å and $\Delta_X = \frac{|w_X - w_m|}{w_m}$ is the relative difference -in per cent- between the theoretical value X and the measured one.

Transition	$T(10^4$ K)	$N_e(10^{17}$ cm$^{-3})$	w_Q	w_m	Δ_Q	$\Delta_{G(MSE)}$	$\Delta_{G(SMSE)}$
3s3d ^{3}D$_3$–3s4p ^{3}P°$_2$	1.88	1.00	0.184	0.311[a]	41	44	45
λ = 308.624 nm	1.50	1.45	0.293	0.306*	4.2	7.4	9.9
3s3d ^{3}D$_2$–3s4p ^{3}P°$_1$	1.88	1.00	0.189	0.285[a]	34	39	40
λ = 309.342 nm	1.50	1.45	0.301	0.319*	5.6	12	13
3s3d ^{3}D$_1$–3s4p ^{3}P°$_0$	4.80	2.60	0.347	0.290[b]	20	2.0	3.8
λ = 309.683 nm	4.90	1.40	0.185	0.168[b]	10	9.1	12
	5.00	1.70	0.224	0.194[b]	15	5.7	8.3
	1.88	1.00	0.188	0.277[a]	32	37	38
	1.50	1.45	0.300	0.332*	9.6	15	16
3s4s ^{3}S$_1$–3s4p ^{3}P°$_1$	0.87	1.00	0.622	0.48[c]	30	69	92
λ = 455.262 nm	1.06		0.578	0.42[c]	38	75	100
	1.28		0.539	0.40[c]	35	67	89
	1.64		0.494	0.38[c]	30	56	75
	2.56	0.58	0.247	0.180[d]	37	52	72
	1.90	1.00	0.470	0.53[e]	11	3.1	18
	1.90	1.00	0.470	0.512[a]	8.2	7.5	22
	1.50	1.45	0.739	0.756*	2.2	19	33
3s4s ^{3}S$_1$–3s4p ^{3}P°$_0$	0.87	1.00	0.629	0.56[c]	12	45	64
λ = 456.782 nm	2.56	0.58	0.250	0.181[d]	38	52	72
	1.90	1.00	0.475	0.50[e]	5.0	9.9	25
	1.90	1.00	0.475	0.542[a]	12	2.0	15
	1.50	1.45	0.747	0.784*	4.7	15	30
3s4s ^{3}S$_1$–3s4p ^{3}P°$_2$	2.56	0.58	0.251	0.176[d]	43	56	79
λ = 457.476 nm	2.30	1.00	0.448	3.06[f]	85	84	81
	1.90	1.00	0.477	0.50[e]	4.6	11	25
	1.90	1.00	0.477	0.485[a]	1.6	14	30
	1.50	1.45	0.750	0.791*	5.2	14	30
3s4s ^{1}S$_0$–3s4p ^{1}P°$_1$	2.30	1.00	0.818	0.71[f]	15	20	35
λ = 537.973 nm	1.90	1.00	0.875	0.87[e]	0.57	8.7	22
	1.90	1.00	0.875	0.982[a]	11	3.8	7.5
	1.50	1.45	1.382	1.346*	2.7	15	28
3s4p ^{3}P°$_0$–3s4d ^{3}D$_1$	2.56	0.58	0.204	0.204[d]	0.0	47	39
λ = 379.141 nm	2.30	1.00	0.369	0.37[f]	0.27	47	39
	1.90	1.00	0.404	0.68[e]	41	14	17
	1.88	1.00	0.406	0.743[a]	45	21	24
	1.50	1.45	0.655	1.028*	36	8.3	9.9
3s4p ^{3}P°$_1$–3s4d ^{3}D$_2$	2.30	1.00	0.371	0.48[f]	23	12	7.5
λ = 379.611 nm	1.90	1.00	0.406	0.68[e]	40	14	17
	1.88	1.00	0.408	0.797[a]	49	26	29
	1.50	1.45	0.658	0.962*	32	0.99	3.8
3s4p ^{3}P°$_2$–3s4d ^{3}D$_3$	2.30	1.00	0.536	0.47[f]	14	16	9.9
λ = 380.654 nm	1.90	1.00	0.584	0.69[e]	15	15	17
	4.80	2.60	0.997	1.184[g]	16	9.9	21
	4.90	1.40	0.532	0.726[g]	27	22	32
	5.00	1.70	0.640	0.992[g]	35	31	40
	1.88	1.00	0.587	0.784[a]	25	24	27
	1.50	1.45	0.945	1.043*	9.4	8.3	11
3s4p ^{1}P°$_1$–3s4d ^{1}D$_2$	2.30	1.00	0.539	0.54[f]	0.19	33	7.4
λ = 359.047 nm	1.88	1.00	0.590	0.866[a]	32	11	36
	1.50	1.45	0.947	1.235*	23	0.99	27
3s4f ^{1}F°$_3$–3s5g ^{1}G$_4$	4.80	2.60	1.132	1.634[g]	31	61	59
λ = 392.447 nm	4.90	1.40	0.604	0.918[g]	34	54	61
	5.00	1.70	0.726	1.106[g]	34	56	61
	1.90	1.00	0.674	0.846[a]	20	52	51
	1.50	1.45	1.095	1.719*	36	18	61

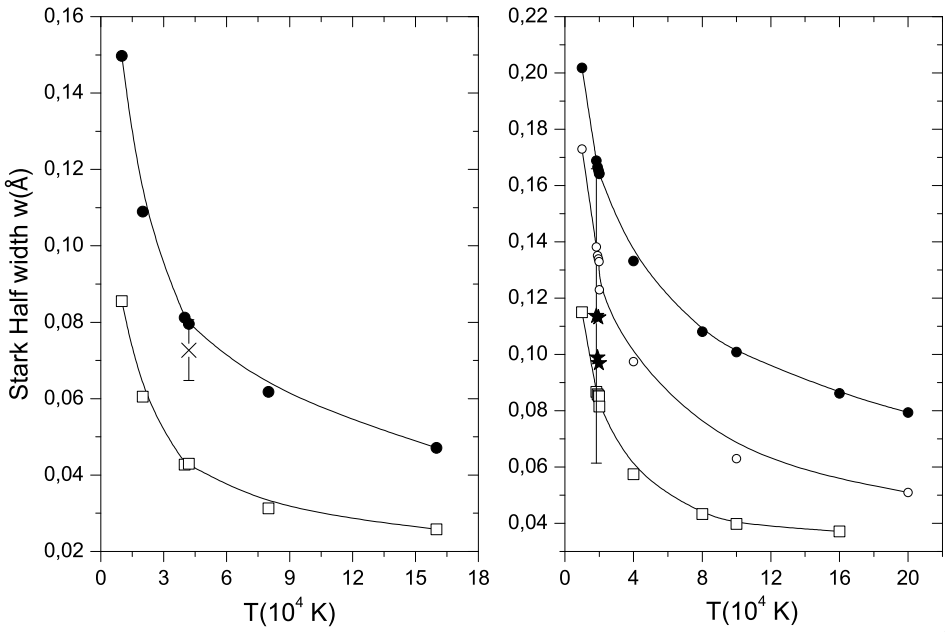

Figure 3. Stark HWHM for the two O III lines: $2p(^2P^o)3s\ ^3P^o_1 - 2p(^2P^o)3p\ ^3D_2$ (left panel) and $2p(^2P^o)3p\ ^3S_1 - 2p(^2P^o)3d\ ^3P^o_0$ (right panel) as a function of temperature and normalized to electron density $N_e = 10^{17}$ cm^{-3}. •: present calculations, □: D(MSE) (Dimitrijević 1988), ○: SCP (Srećković et al. 2001b; Dimitrijević et al. 2011), ×: experimental results of Srećković et al. (2005) and ⋆: experimental results of Blagojević et al. (2000).

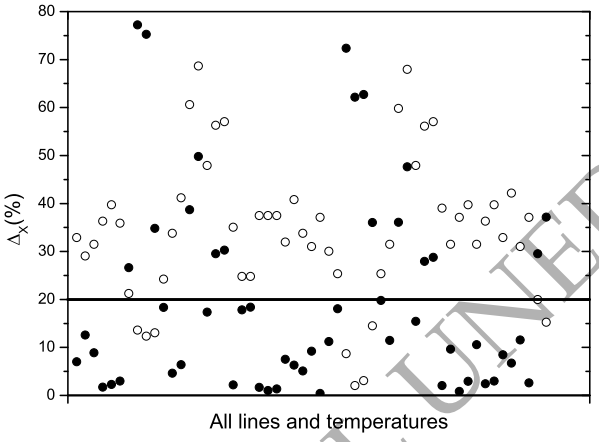

Figure 4. Relative errors Δ_X as defined in Table 4 of some Si II lines between the experimental results w_m and the quantum Δ_Q (present calculations): • and the simplified modified semi empirical ones $\Delta_{G(SMSE)}$ performed in Gavanski et al. (2016): ○. The experimental results are those indicated in Table 4.

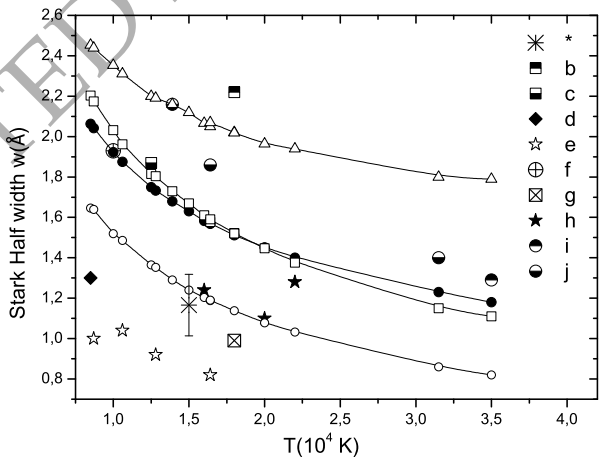

Figure 5. Stark HWHM w in Å of the Si II $3s^24s\ ^2S_{1/2} - 3s^24p\ ^2P^\circ_{1/2}$ line as a function of temperature at an electron density 10^{17} cm^{-3}. The symbols indicated on the Figure are those of the experimental results taken from Table 4. The theoretical results are: the present quantum : •, the semi classical (Griem 1974): △, the modified semi empirical G(MSE): □ and the simplified modified semi empirical ones G(SMSE)): ○. The G(MSE) and G(SMSE) results are obtained in Gavanski et al. (2016).

3.5 Results for Al III

The electronic configurations used for the calculation of the Al III Stark widths are $1s^22s^22p^6$(3s, 3p, 3d, 4s, 4p, 4d, 4f, 5s) giving rise to 13 fine structure levels. The scaling parameters from the SST code are $\lambda_s = 1.0975$, $\lambda_p = 1.0043$, $\lambda_d = 0.8642$ and $\lambda_f = 0.8020$. We calculated the Stark HWHM of 17 Al III lines and we display them in Table 6. Since there are no experimental results for these lines, our quantum widths w_Q are compared to the modified semi empirical (MSE) results of Dimitrijević (1988), and to the semi classical perturbation (SCP) results of (Dimitrijević & Sahal-Bréchot 1993). We find that the average ratio Q/SCP is about 1.6

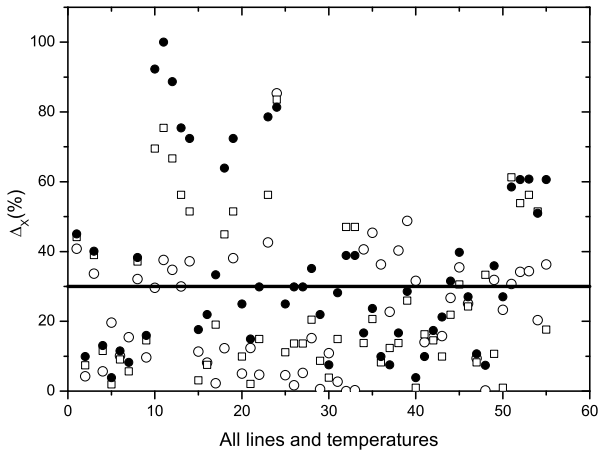

Figure 6. Relative errors Δ_X as defined in Table 5 of some Si III lines between the experimental results w_m and the quantum Δ_Q (present calculations): •, modified semi empirical $\Delta_{G(MSE)}$: □ and the simplified modified semi empirical ones $\Delta_{G(SMSE)}$: ○. The experimental results are those indicated in Table 5. G(MSE) and G(SMSE) are calculated by Gavanski et al. (2016).

and that of the MSE results Q/MSE is about 2.5. Table 7 displays Stark HWHM of 8 other Al III lines for which experimental results exist. Our quantum widths w_Q, the MSE (Dimitrijević 1988), and the SCP (Dimitrijević & Sahal-Bréchot 1993) ones are compared to the only available measured Stark widths of Dojić et al. (2020). The MSE values have been taken from the database STARK-B (Sahal-Bréchot et al. 2022). Our quantum results are overestimated compared to the experimental ones for almost all the considered lines. The average difference between the two results is 40 per cent, with a huge difference for the resonance line 4s $^2S_{1/2}$–4p $^2P^\circ_{1/2}$ (73 per cent). Contrary to our quantum results, the MSE and the SCP show an acceptable agreement with the experimental results (respectively 6 and 17 per cent). A similar conclusion has been previously found for the O III line widths in subsection 3.2.

To explain this disagreement, we investigate the behaviour of the Stark width with temperature. So, we plot in Figure 8 our quantum Stark HWHM for two chosen Al III lines: 4s $^2S_{1/2}$–4p $^2P^\circ_{1/2}$ and 4p $^2P^\circ_{3/2}$–4d $^2D_{3/2}$, together with the semi classical perturbation (Dimitrijević & Sahal-Bréchot 1993) and the modified semi empirical results (Dimitrijević & Konjević 1980). Widths are presented as a function of electron temperature and at an electron density $N_e = \times 10^{17}$ cm^{-3}. We see that the disagreement between our quantum results and the semi classical ones is important for low temperatures: a potential reason of this disagreement is the contributions of elastic and strong (close) collisions to Stark broadening, which become dominant at low temperatures. In fact, we have shown (Elabidi 2021b) that the evaluation of these contributions is different in quantum and semi classical approaches, and the semi classical method does not correctly estimate these contributions. We have shown also in Aloui et al. (2018) that, at low temperature, the contributions of elastic collisions are important compared to the inelastic ones, and this may affect the Stark widths. To confirm this conclusion, we investigate the behaviour of the contributions of strong and elastic collisions to the Stark broadening of the transition 4p $^2P^\circ_{1/2}$–4d $^2D_{3/2}$ with temperature. These results are presented in Table 8. We see that these two contributions decrease with temperature, and at the same time the agreement between the quantum and the semi classical results becomes better. This has been well confirmed in the Figure 9, where the ratio Q/SCP of the quantum and semi classical results decreases and reaches one when the contributions of strong and elastic collisions to the total Stark width decrease.

4 CONCLUSION

We have calculated in the present work Stark Half Widths at Half intensity Maximum (HWHM) of 64 lines of the ions O II, Si II, Si III and Al III. These widths have been measured long time ago (since 1974), but new experiments have been recently performed (Gavanski et al. (2016) for O II, Si II and Si III, and Dojić et al. (2020) for Al III). The number of the experiments considered in the present work is relatively high to be very satisfying for some conclusions: from 7 to 10 different experiments for each ion from the older (Konjević et al. 1970) to the more recent ones (Gavanski et al. 2016; Dojić et al. 2020). The Stark widths have been also calculated using different approaches (semi classical perturbation, modified and simplified modified semi empirical), except the quantum ones. Although the number of evaluations of the Stark widths of these ions is high, the experimental and the theoretical results still slightly dispersed and the difference between them is relatively wide in several cases. This dispersion is an obstacle to make a decision about the accuracy of the results. That is why, we present here the first quantum mechanical calculations for these ions: 35 lines of O II, 9 lines of Si II, 12 lines of Si III and 8 lines of Al III, hoping that these calculations help us to decide about the accuracy of the available results, since the quantum method has been applied many times before and has shown the best agreement with different experimental results, so, we can say that it is supposed to be more accurate than the other approaches.

For the O II ion, our quantum calculations present the better agreement with the experimental results together with the semi classical ones (Griem 1974): the average error is about 9 per cent, and the majority of the results agree within 15 per cent with the measurements. The modified semi empirical G(MSE) results obtained in Gavanski et al. (2016) present an average error of about 35 per cent, and the simplified modified semi empirical G(SMSE) ones (Gavanski et al. 2016) agree within 50 per cent with the experimental results. For the Si II ion, the average relative difference between our quantum results and the experimental ones is about 25 per cent. They are also the most close to the experimental results compared to the theoretical results involved in this study: the relative error is about 40 per cent for the semi classical (Griem 1974) results, and 30 per cent for the results of (Gavanski et al. 2016) obtained using the modified semi empirical method G(MSE). We find that 70 per cent of our quantum Stark widths (for all the temperature values) have relative errors less than 20 per cent with the experimental results. The widths of 20 lines of the O III ion have been calculated in the present work. Our quantum results for 13 lines have been compared to the available experimental results of Platiša et al. (1975); Blagojević et al. (2000); Srećković et al. (2001b, 2005). An acceptable agreement (17 per cent) has been found with the newer measurements of Srećković et al. (2005). The relative error with the results of Blagojević et al. (2000) is about 48 per cent. The D(MSE) results are however closer to the experimental results of Blagojević et al. (2000) ($\Delta_{D(MSE)}$ = 20 per cent), while they present a difference of 44 per cent with the Srećković et al. (2005) results. If we average over all the lines and all the temperature val-

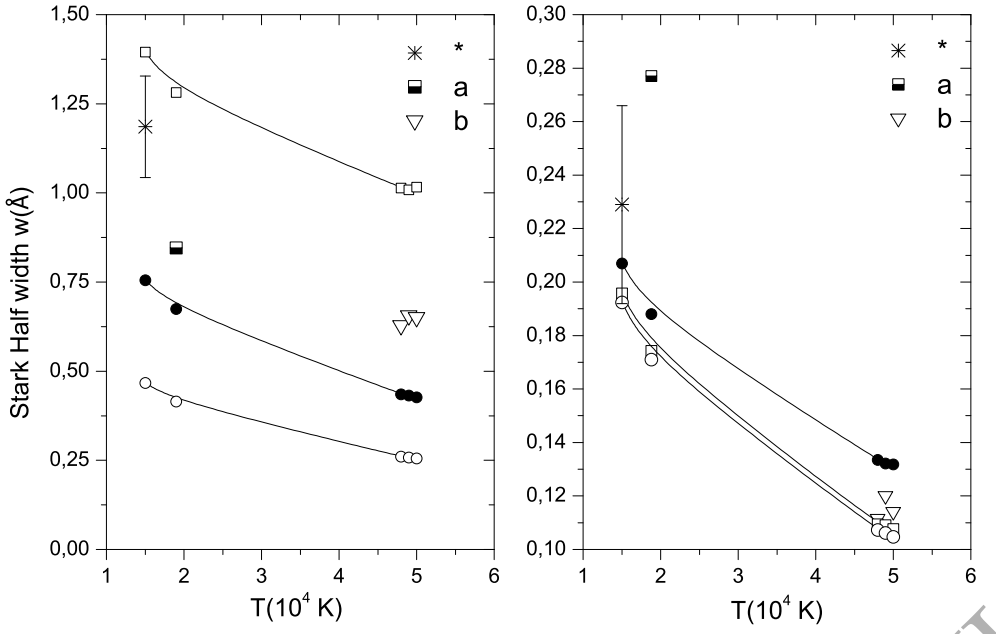

Figure 7. Stark HWHM w in Å for the Si III 3s4f ^{1}F°$_3$−3s5g ^{1}G$_4$ (left) and 3s3d ^{3}D$_1$−3s4p ^{3}P°$_0$ (right) lines as a function of temperature at an electron density 10^{17} cm^{-3}. The symbols indicated on the Figure are those of the experimental results taken from Table 5. The theoretical results are: the present quantum : •, the modified semi empirical (Gavanski et al. 2016): □ and the simplified modified semi empirical ones (Gavanski et al. 2016): ○.

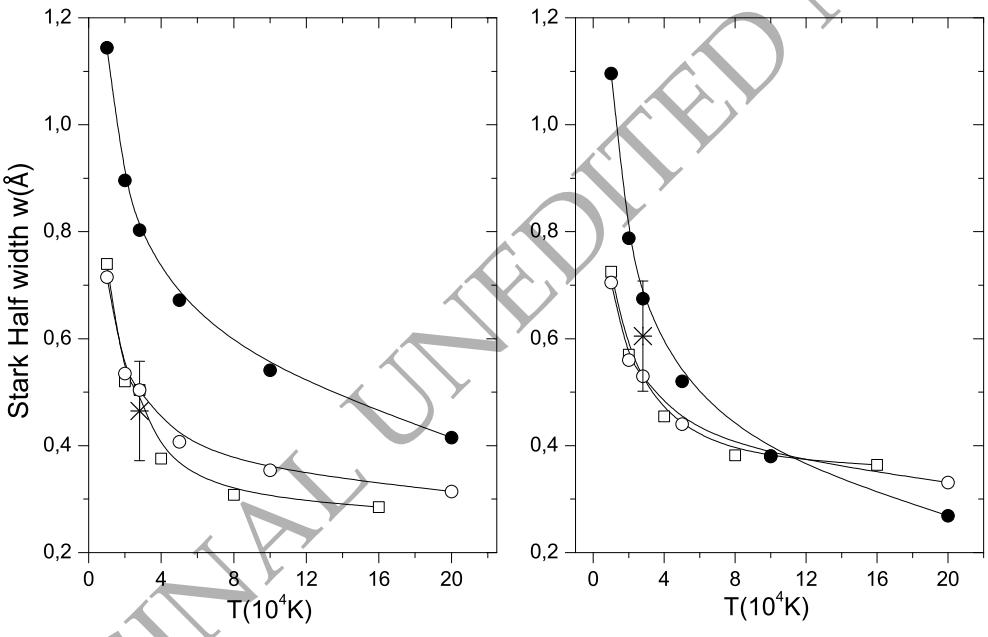

Figure 8. Stark HWHM w in Å for the two Al III lines: 4s ^{2}S$_{1/2}$−4p ^{2}P°$_{1/2}$ (left panel) and 4p ^{2}P°$_{1/2}$−4d ^{2}D$_{3/2}$ (right panel) as a function of temperature at an electron density 10^{17} cm^{-3}. The present quantum results •, the semi classical perturbation (Dimitrijević & Sahal-Bréchot 1993): ○, and the modified semi empirical results (Dimitrijević 1988): □ are compared to the experimental results of Dojić et al. (2020).

Table 6. Present quantum Stark HWHM w_Q in Å for Al III lines compared to the modified semi empirical (Dimitrijević 1988): MSE and to the semi classical perturbation (Dimitrijević & Sahal-Bréchot 1993): SCP results at an electron density $N_e = 10^{17}$ cm^{-3}.

Transition	$T(10^4$ K)	w_Q	$w_{\rm SCP}$	$w_{\rm MSE}$	$\frac{w_Q}{w_{\rm SCP}}$	$\frac{w_Q}{w_{\rm MSE}}$
$3s\ ^2S_{1/2}-4p\ ^2P^o_{3/2}$	1	0.0225	0.0082	0.0068	2.74	3.31
$\lambda = 69.583$ nm	2	0.0159	0.0061	0.0048	2.61	3.31
	4	0.0114	0.0051	0.0034	2.24	3.35
	10	0.0073	0.0038	0.0026	1.92	2.81
$3s\ ^2S_{1/2}-4p\ ^2P^o_{1/2}$	1	0.0227			2.77	3.34
$\lambda = 69.622$ nm	2	0.0161			2.64	3.35
	4	0.0115			2.25	3.38
	10	0.0073			1.92	2.81
$3p\ ^2P^o_{1/2}-5s\ ^2S_{1/2}$	1	0.0232	0.0206	–	1.13	
$\lambda = 85.503$ nm	2	0.0166	0.0158	–	1.05	
	4	0.0119	0.0120	–	0.99	
	10	0.0078	0.0115	–	0.68	
$3p\ ^2P^o_{3/2}-5s\ ^2S_{1/2}$	1	0.0233		–	1.13	
$\lambda = 85.567$ nm	2	0.0166		–	1.05	
	4	0.0119		–	0.99	
	10	0.0078		–	0.68	
$3p\ ^2P^o_{1/2}-4d\ ^2D_{3/2}$	1	0.0371	0.0246	–	1.51	
$\lambda = 89.202$ nm	2	0.0263	0.0193	–	1.36	
	4	0.0188	0.0167	–	1.13	
	10	0.0120	0.0123	–	0.98	
$3p\ ^2P^o_{3/2}-4d\ ^2D_{3/2}$	1	0.0372		–	1.51	
$\lambda = 89.389$ nm	2	0.0263		–	1.36	
	4	0.0188		–	1.13	
	10	0.0120		–	0.98	
$3p\ ^2P^o_{3/2}-4d\ ^2D_{5/2}$	1	0.0364		–	1.48	
$\lambda = 89.390$ nm	2	0.0257		–	1.33	
	4	0.0184		–	1.10	
	10	0.0116		–	0.94	
$3p\ ^2P^o_{1/2}-4s\ ^2S_{1/2}$	1	0.0737	0.0291	–	2.53	
$\lambda = 137.967$ nm	2	0.0531	0.0208	–	2.55	
	4	0.0386	0.0166	–	2.33	
	10	0.0255	0.0116	–	2.20	
$3p\ ^2P^o_{3/2}-4s\ ^2S_{1/2}$	1	0.0741		–	2.55	
$\lambda = 138.413$ nm	2	0.0534		–	2.57	
	4	0.0388		–	2.34	
	10	0.0257		–	2.22	
$3p\ ^2P^o_{1/2}-3d\ ^2D_{3/2}$	1	0.0405	0.0226	0.0158	1.79	2.56
$\lambda = 160.577$ nm	2	0.0292	0.0164	0.0112	1.78	2.61
	4	0.0216	0.0129	0.0079	1.67	2.73
	10	0.0150	0.0083	0.0048	1.81	3.13
$3p\ ^2P^o_{3/2}-3d\ ^2D_{3/2}$	1	0.0408			1.81	2.58
$\lambda = 161.181$ nm	2	0.0294			1.79	2.63
	4	0.0217			1.68	2.75
	10	0.0151			1.82	3.15
$3p\ ^2P^o_{3/2}-3d\ ^2D_{5/2}$	1	0.0399			1.77	2.53
$\lambda = 161.187$ nm	2	0.0288			1.76	2.57
	4	0.0213			1.65	2.70
	10	0.0148			1.78	3.08
$3s\ ^2S_{1/2}-3p\ ^2P^o_{3/2}$	1	0.0480	0.0260	0.0152	1.85	3.16
$\lambda = 185.472$ nm	2	0.0346	0.0186	0.0107	1.86	3.23
	4	0.0254	0.0146	0.0076	1.74	3.34
	10	0.0174	0.0090	0.0048	1.93	3.63
$3s\ ^2S_{1/2}-3p\ ^2P^o_{1/2}$	1	0.0485			1.87	3.19
$\lambda = 186.279$ nm	2	0.0350			1.88	3.27
	4	0.0256			1.75	3.37
	10	0.0176			1.96	3.67

Table 6. *Continued.*

Transition	$T(10^4$ K)	w_Q	$w_{\rm SCP}$	$w_{\rm MSE}$	$\frac{w_Q}{w_{\rm SCP}}$	$\frac{w_Q}{w_{\rm MSE}}$
3d ^{2}D$_{5/2}$–4f ^{2}F$^{\rm o}_{7/2}$	1	0.1128	0.0960	0.0740	1.18	1.52
λ = 193.584 nm	2	0.0797	0.0735	0.0605	1.08	1.32
	4	0.0565	0.0604	0.0499	0.94	1.13
	10	0.0362	0.0445	0.041	0.81	0.88
3d ^{2}D$_{5/2}$–4f ^{2}F$^{\rm o}_{5/2}$	1	0.1160			1.21	1.57
λ = 193.586 nm	2	0.0819			1.11	1.35
	4	0.0580			0.96	1.16
	10	0.0371			0.83	0.90
3d ^{2}D$_{3/2}$–4f ^{2}F$^{\rm o}_{5/2}$	1	0.1154			1.20	1.56
λ = 193.596 nm	2	0.0815			1.11	1.35
	4	0.0577			0.96	1.16
	10	0.0370			0.83	0.90

Table 7. Stark HWHM in Å for other Al III lines: present quantum results $w_{\rm Q}$, the SCP (Dimitrijević & Sahal-Bréchot 1993) and the MSE (Dimitrijević 1988) ones are compared to the experimental results w_m of Dojić et al. (2020). Values are normalized to $N_e = 10^{17}$ cm^{-3}.

Transition	$T(10^4$ K)	w_Q	w_m	$w_{\rm SCP}$	$w_{\rm MSE}$	Δ_Q	$\Delta_{\rm SCP}$	$\Delta_{\rm MSE}$
3d ^{2}D$_{5/2}$–4p ^{2}P$^{\rm o}_{3/2}$	1	0.384		0.217	–			
λ = 360.16 nm	2	0.287		0.164	–			
	2.8	0.252	0.19	0.153	–	33	19	
	8	0.172		0.110	–			
	10	0.159		0.103	–			
3d ^{2}D$_{3/2}$–4p ^{2}P$^{\rm o}_{1/2}$	1	0.394			–			
λ = 360.24 nm	2	0.294			–			
	2.8	0.258	0.175		–	47	19	
	8	0.177			–			
	10	0.163			–			
4p ^{2}P$^{\rm o}_{1/2}$–5s ^{2}S$_{1/2}$	1	0.461		0.454	–			
λ = 370.21 nm	2	0.341		0.355	–			
	2.8	0.298	0.555	0.293	–	46	47	
	8	0.200		0.259	–			
	10	0.180		0.249	–			
4p ^{2}P$^{\rm o}_{3/2}$–5s ^{2}S$_{1/2}$	1	0.464			–			
λ = 371.31 nm	2	0.343			–			
	2.8	0.300	0.585		–	49	47	
	8	0.200			–			
	10	0.184			–			
4p ^{2}P$^{\rm o}_{1/2}$–4d^{2}D$_{3/2}$	1	1.096		0.705	0.725			
λ = 451.26 nm	2	0.788		0.560	0.570			
	2.8	0.675	0.605	0.529	0.527	12	13	13
	8	0.421		0.406	0.382			
	10	0.380		0.381	0.377			
4p ^{2}P$^{\rm o}_{3/2}$–4d^{2}D$_{3/2}$	1	1.099						
λ = 452.92 nm	2	0.790						
	2.8	0.676	0.670			1	13	13
	8	0.422						
	10	0.381						
4s ^{2}S$_{1/2}$–4p ^{2}P$^{\rm o}_{3/2}$	1	1.133		0.715	0.740			
λ = 569.66 nm	2	0.887		0.535	0.520			
	2.8	0.795	0.500	0.500	0.467	59	0	7
	8	0.575		0.377	0.308			
	10	0.534		0.354	0.299			
4s ^{2}S$_{1/2}$–4p ^{2}P$^{\rm o}_{1/2}$	1	1.144						
λ = 572.27 nm	2	0.896						
	2.8	0.803	0.465			73	0	7
	8	0.582						
	10	0.541						

Table 8. Contribution of strong ($\frac{Strong}{Total}$) and elastic ($\frac{Elastic}{Total}$) collisions to the total semi classical perturbation (SCP) Stark widths as a function of electron temperature for the Al III 4p ^{2}P°$_{1/2}$–4d ^{2}D$_{3/2}$ line. w_Q and w_{SCP} are respectively the quantum and the semi classical perturbation Stark widths.

$T(10^4$ K)	$\frac{Elastic}{Total}$	$\frac{Strong}{Total}$	$\frac{w_Q}{w_{SCP}}$
1	0.64	0.35	1.56
1.5	0.59	0.37	1.48
2	0.59	0.37	1.41
2.8	0.56	0.37	1.27
5	0.51	0.32	1.18
10	0.45	0.31	1.00

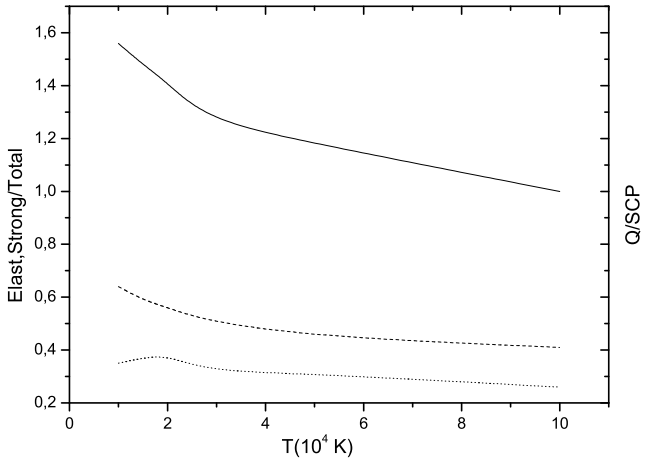

Figure 9. Ratios $\frac{Elast}{Total}$ (- - -) and $\frac{Strong}{Total}$ (. . .) of the elastic and strong collision contributions to the total Stark widths as a function of electron temperature together with the ratio $\frac{Q}{SCP}$ (—) of our quantum to the semi classical perturbation results for the Al III 4p ^{2}P°$_{1/2}$–4d ^{2}D$_{3/2}$ line.

ues, we find that our quantum results, the D(MSE) and the SCP ones agree with the experimental results within about 30 per cent. The quantum results of the Si III ion still presenting the best agreement with the experimental ones, but with slightly higher relative error (22 per cent) compared to the two precedent ions. The corresponding relative errors for the G(MSE) and the G(SMSE) results obtained in (Gavanski et al. 2016) are respectively 27 and 35 per cent. The best agreement of our quantum results occurs with the new experiments of Gavanski et al. (2016). The case of the Al III ion is slightly different from the three precedent ones: our quantum results present the higher disagreement with the experimental ones of Dojić et al. (2020), the average relative error is about 40 per cent. However, the modified semi empirical (Dimitrijević 1988) and the semi classical perturbation (Dimitrijević & Sahal-Bréchot 1993) approaches agree well with the measurements. We tried to explain this exceptional difference between the experimental and our quantum results by investigating the contributions of elastic and strong collisions to Stark widths. These contributions are evaluated differently in quantum and semi classical approaches, and we have shown that when these contributions are important (at low temperature), the disagreement between the two approaches increases. We recall that the SCP method underestimates the elastic and strong

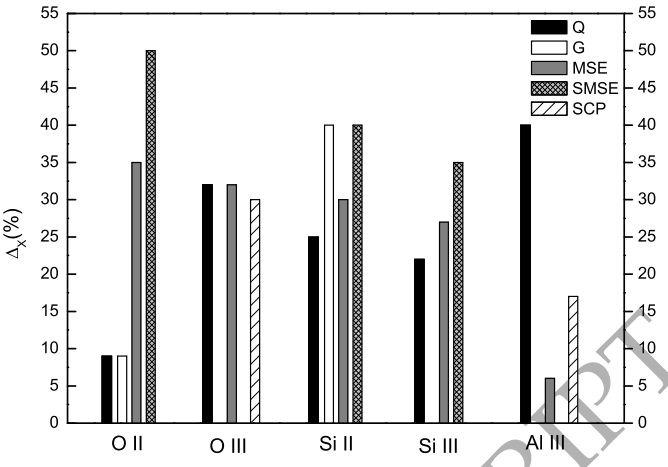

Figure 10. Average relative errors Δ_X between the experimental results on one hand and the other theoretical ones: our quantum (Q), the semi classical (Gr) (Griem 1974). The modified semi empirical G(MSE), and the simplified modified semi empirical G(SMSE) results for the three ions O II, Si II and Si III are obtained in Gavanski et al. (2016), the D(MSE) results of O III and Al III are obtained in Dimitrijević (1988). The semi classical perturbation results (SCP) for O III are obtained in Dimitrijević et al. (2011); Srećković et al. (2001b), and those of Al III are obtained in Dimitrijević & Sahal-Bréchot (1993).

collision contributions to the Stark widths. Figure 10 recapitulates the relative errors between the results of the theoretical calculations: Q, G(MSE), G(MSE), G, SCP and the experimental results of the four considered ions.

We hope that the new quantum Stark widths could be of interest in stellar-atmosphere modelling, and could be used with confidence in plasma diagnostic. The obtained quantum results will be implemented to the database STARK-B (Sahal-Bréchot et al. 2022). As it was recommended in Gavanski et al. (2016), new experiments and calculations for the considered lines are welcome to reach a conclusion, especially for the Al III ion for which we found only one experiment.

DATA AVAILABILITY

The data underlying this article are available in the article.

ACKNOWLEDGMENTS

The authors extend their appreciation to the Deputyship for Research & Innovation, Ministry of Education in Saudi Arabia for funding this research work through the project number : IFP22UQU4331237DSR236.
This work has been supported by the Tunisian Laboratory of Molecular Spectroscopy and Dynamics LR18ES02 and the French Research Unit UMR8112, and by the Paris Observatory and the CNRS. We also acknowledge financial support from the 'Programme National de Physique Stellaire' (PNPS) of CNRS/INSU, CEA and CNES, France.

REFERENCES

Aloui R., Elabidi H., Sahal-Bréchot S., Dimitrijević M., 2018, Atoms, 6, 20
Aloui R., Elabidi H., Sahal-Bréchot S., 2019a, J. Quant. Spectrosc. Radiat. Transfert, 239, 106675
Aloui R., Elabidi H., Hamdi R., Sahal-Bréchot S., 2019b, MNRAS, 484, 4801
Aloui R., Elabidi H., Sahal-Bréchot S., 2022, MNRAS, 484, 4801
Arellano Ferro A., Giridhar S., Mathias P., 2001, A&A, 368, 250
Baranger M., 1958, Phys. Rev., 111, 481
Ben Nessib N., Elabidi H., Cornille M., Dubau J., 2005, Phys. Scr., 72, 23
Blagojević B., Popović M. V., Konjević N., 1999, Phys. Scr., 59, 374
Blagojević B., Popović M. V., Konjević N., 2000, J. Quant. Spectrosc. Radiative Transfer, 67, 9
Bukvić S., Djeniže S., Srećković A., 2009, A&A, 508, 491
Chan L. Y., Mostovych A. N., Kearney K. J., 1996, J. Quant. Spectrosc. Radiative Transfer, 55, 815
Chiang W. T., Griem H. R., 1978, Phys. Rev. A, 18, 1169
Cowley C. R., 1971, The Observatory, 91, 139
Cuesta L., Phillips J. P., 2000, ApJ, 543, 754
Del Val J. A., Aparicio J. A., González V., Mar S., 1999, A&AS, 140, 171
Dimitrijević M. S., 1988, A&AS, 76, 53
Dimitrijević M. S., 2003, Astronomical & Astrophysical Transactions, 22, 389
Dimitrijević M. S., 2020, Data, 5, 1
Dimitrijević M. S., Konjević N., 1980, J. Quant. Spectrosc. Radiative Transfer, 24, 451
Dimitrijević M. S., Konjević N., 1987, A&A, 172, 345
Dimitrijević M. S., Sahal-Bréchot S., 1993, A&AS, 99, 585
Dimitrijevic M. S., Feautrier N., Sahal-Brechot S., 1981, Journal of Physics B Atomic Molecular Physics, 14, 2559
Dimitrijević M. S., Kovačević A., Simić Z., Sahal-Bréchot S., 2011, Baltic Astronomy, 20, 580
Djeniže S., Srećković A., Labat J., Platiša M., 1991, Zeitschrift fur Physik D Atoms Molecules Clusters, 21, 295
Djeniže S., Srećković A., Labat J., Purić J., Platiša M., 1992, Journal of Physics B Atomic Molecular Physics, 25, 785
Djeniže S., Milosavljević V., Srećković A., 1998, J. Quant. Spectrosc. Radiative Transfer, 59, 71
Djurović S., Nikolić D., Savić I., Sörge S., Demura A. V., 2005, Phys. Rev. E, 71, 036407
Djurović S., Ćirišan M., Demura A. V., Demchenko G. V., Nikolić D., Gigosos M. A., González M. Á., 2009, Phys. Rev. E, 79, 046402
Djurović S., Mijatović Z., Vujičić B., Kobilarov R., Savić I., Gavanski L., 2015, Physics of Plasmas, 22, 013505
Dojić D., Skočić M., Bukvić S., Djeniže S., 2020, Spectrochimica Acta, 166, 105816
Eissner W., 1998, Comput. Phys. Commun., 114, 295
Eissner W., Jones M., Nussbaumer H., 1974, Comput. Phys. Commun., 8, 270
Elabidi H., 2021a, J. Quant. Spectrosc. Radiative Transfer, 259, 107407
Elabidi H., 2021b, MNRAS, 503, 5730
Elabidi H., Sahal-Bréchot S., 2013, MNRAS, 436, 1452
Elabidi H., Sahal-Bréchot S., 2018, MNRAS, 480, 697
Elabidi H., Sahal-Bréchot S., 2019, MNRAS, 484, 1072
Elabidi H., Ben Nessib N., Sahal-Bréchot S., 2004, J. Phys. B: At. Mol. Opt. Phys., 37, 63
Elabidi H., Ben nessib N., Cornille M., Dubau J., Sahal-Bréchot S., 2008, J. Phys. B: At. Mol. Opt. Phys., 41, 025702
Elabidi H., Ben Nessib N., Sahal-Bréchot S., 2009, Eur. Phys. J. D, 54, 51
Elabidi H., Sahal-Bréchot S., Ben Nessib N., 2012, Phys. Scr., 85, 065302
Elabidi H., Sahal-Bréchot S., Dimitrijević M. S., 2014, Adv. Space Res., 54, 1184
Fleurier C., Sahal-Bréchot S., Chapelle J., 1977, Journal of Physics B Atomic Molecular Physics, 10, 3435
Gailitis M., 1963, J. Exptl. Theoret. Phys., 17, 1328
Gavanski L., Belmonte M. T., Savić I., Djurović S., 2016, MNRAS, 457, 4038
Gigosos M. A., Djurović S., Savić I., González-Herrero D., Mijatović Z., Kobilarov R., 2014, A&A, 561, A135
Glagolevskij Y. V., Leushin V. V., Chuntonov G. A., Shulyak D., 2006, Astronomy Letters, 32, 54
González V. R., Aparicio J. A., del Val J. A., Mar S., 2002, Journal of Physics B Atomic Molecular Physics, 35, 3557
Griem H. R., 1968, Physical Review, 165, 258
Griem H. R., 1974, Spectral line broadening by plasmas. Academic Press, New York
Hamdi R., Ben Nessib N., Sahal-Bréchot S., Dimitrijević M. S., 2021, MNRAS, 504, 1320
Hartquist T. W., Snijders M. A. J., West K. A., 1983, MNRAS, 203, 1183
Iglesias C. A., Rogers F. J., Wilson B. G., 1990, ApJ, 360, 221
Ivković M., Gonzalez M. A., Jovićević S., Gigosos M. A., Konjević N., 2010, Spectrochimica Acta, 65, 234
Khalack V., Landstreet J. D., 2012, MNRAS, 427, 569
Konjević N., Purić J., Ćirković L. J., Labat J., 1970, Journal of Physics B Atomic Molecular Physics, 3, 999
Kusch H. J., Schroeder K., 1982, A&A, 116, 255
Lambert D. L., Warner B., 1968, MNRAS, 138, 213
Lesage A., Miller M., 1975, Academie des Sciences Paris Comptes Rendus Serie B Sciences Physiques, 280, 645
Lesage A., Redon R., 2004, A&A, 418, 765
Lesage A., Sahal-Bréchot S., Miller M. H., 1977, Phys. Rev. A, 16, 1617
Lesage A., Rathore B. A., Lakićević I. S., Purić J., 1983, Phys. Rev. A, 28, 2264
Lorenzo J., Negueruela I., Castro N., Norton A. J., Vilardell F., Herrero A., 2014, A&A, 562, A18
Muzzin A., et al., 2012, ApJ, 746, 188
Nelson C. H., 2000, ApJ, 544, L91
Pérez C., de La Rosa I., de Frutos A., Mar S., 1990, in Frommhold L., Keto J. W., eds, American Institute of Physics Conference Series Vol. 216, Spectral line shapes. pp 67–68, doi:10.1063/1.39874
Pérez C., de La Rosa I., de Frutos A. M., Mar S., 1993, Phys. Rev. E, 47, 756
Platiša M., Popović M. V., Konjeyić N., 1975, A&A, 45, 325
Platiša M., Dimitrijević M., Popović M., Konjević N., 1977, Journal of Physics B Atomic Molecular Physics, 10, 2997
Pretty W. E., 1931, Proceedings of the Physical Society, 43, 279
Purić J., Djeniže S., Labat J., Ćirković L., 1973, Physics Letters A, 45, 97
Purić J., Djeniže S., Labat J., Ćirković L. J., 1974, Zeitschrift fur Physik, 267, 71
Purić J., Djeniže S., Srećković A., Platiša M., Labat J., 1988, Phys. Rev. A, 37, 498
Rauch T., et al., 2017, A&A, 606, A105
Rauch T., Gamrath S., Quinet P., Demleitner M., Knörzer M., Werner K., Kruk J. W., 2020, A&A, 637, A4
Roberts D., 1968, J. Quant. Spectrosc. Radiative Transfer, 8, 1241
Sahal-Bréchot S., 1969a, A&A, 1, 91
Sahal-Bréchot S., 1969b, A&A, 2, 322
Sahal-Bréchot S., 1974, A&A, 35, 319
Sahal-Bréchot S., 2021, Atoms, 9, 29
Sahal-Bréchot S., Elabidi H., 2021, A&A, 652, A47
Sahal-Bréchot S., Dimitrijević M., Nessib N., 2014, Atoms, 2, 225
Sahal-Bréchot S., Dimitrijević M. S., Moreau N., 2022, STARK-B database, `http://stark-b.obspm.fr`
Saraph H. E., 1978, Comput. Phys. Commun., 15, 247
Sollerman J., et al., 2007, A&A, 466, 839
Srećković A., Drinčić V., Djeniže S., 2001a, Phys. Scr., 63, 306
Srećković A., Dimitrijević M. S., Djeniže S., 2001b, A&A, 371, 354
Srećković A., Bukvić S., Djeniže S., 2005, Phys. Scr., 71, 218
Sun F., et al., 2022, ApJ, 936, L8
Werner K., Rauch T., Knörzer M., Kruk J. W., 2018, A&A, 614, A96
Wollschläger F., Mitsching J., Meiners D., Depiesse M., Richou J., Lesage A., 1997, J. Quant. Spectrosc. Radiative Transfer, 58, 135